12-1-1995

Transients in Power Systems

M. Belkhayat
Purdue University School of Electrical and Computer Engineering

J. Edwards
Purdue University School of Electrical and Computer Engineering

N. Hoonchareon
Purdue University School of Electrical and Computer Engineering

O. Marte
Purdue University School of Electrical and Computer Engineering

D. Stenberg
Purdue University School of Electrical and Computer Engineering

See next page for additional authors

TRANSIENTS IN POWER SYSTEMS

M. BELKHAYAT
J. EDWARDS
N. HOONCHAREON
O. MARTE
D. STENBERG
E. WALTERS

TR-ECE 95-29
DECEMBER 1995

SCHOOL OF ELECTRICAL
AND COMPUTER ENGINEERING
PURDUE UNIVERSITY
WEST LAFAYETTE, INDIANA 47907-1285

Transients in Power Systems

M. Belkhayat
J. Edwards
N. Hoonchareon
O. Marte
D. Stenberg
E. Walters

December, 1995

Preface

Power system engineering largely focuses on steady state analysis. The main areas of power system engineering are power flow studies and fault studies - both steady state technologies. But the world is largely transient, and power systems are always subject to time varying and short lived signals. This technical report concerns several important topics in transient analyses of power systems.

The leading chapter deals with a new analytical tool-wavelets-for power system transients. Flicker and electric are furnace transients are discussed in Chapters II and IV. Chapter III deals with transients from shunt capacitor switching. The concluding chapters deal with transformer inrush current and non simultaneous pole closures of circuit breakers.

This report was prepared by the students in EE532 at Purdue University. When I first came to Purdue in 1965, Professor El-Abiad was asking for student term projects which were turned into technical reports. I have 'borrowed' this idea and for many years we have produced technical reports from the power systems courses. The students get practice in writing reports, and the reader is able to get an idea of the coverage of our courses. I think that the students have done a good job on the subject of transients in power systems.

G. T. Heydt

December 1995

Table of Contents

Chapter I

Wavelet Analysis for Power System Transients

Mohamed Belkhayat

1.1 Introduction

This paper provides an introduction to wavelets and their application for power systems transients. Since wavelets are a relatively new development in engineering, a brief history will be presented for the sake of the uninitiated. An overview of the Integral Wavelet Transform, the Discrete Wavelet Transform, and the wavelet series, which are necessary tools for later discussions, will also be presented. A numerical comparison between the Discrete Wavelet Transform and the Discrete Fourier Transform applied to the identification of a specific class of power transients will be made. Applications in power system transients such as identification, storage, and propagation analysis of transients will then be discussed and the conclusions made.

The earliest recorded development of wavelet functions appears to be in the area of physics. Sixty years ago, a group of physicists studying the details of Brownian motion found out that a set of Harr functions (to be classed as wavelets later on) yielded a better result than the Fourier analysis [1]. After this, Wavelets remained a mathematical curiosity until Grossman and Morlet introduced them in quantum physics in the 1960s. Serious applications in engineering were not considered until the 1980s when Stephan Mallat **[2]** discovered some important relationships between filter banks and the Wavelet Transform. This work, along with the work of Y. Meyer **[3]** and Ingrid Daubechies **[4]** have become the basis for all engineering applications.

It was not until a couple of years ago that researchers such as J. T. Heydt and A. W. Galli [5], Ribiero [6], and D. Robertson [7] introduced wavelets to power systems. One common goal for all of these researchers is to find a better tool to analyze power system transients and their effects on power systems. The ever increasing presence of solid state power loads on the power system grid, such as FACTS, SVCs, DC ties, and rectifier loads causes not only steady state harmonic distortion but significant non-stationary harmonic distortion. The efficient storage of the waveforms resulting from the transients, the identification of these transients, as well as the analysis of the transients propagation are critical areas where wavelet analysis has great potential. The aim of this paper is to discuss these issues and to show where the general trend of the present research is heading.

1.2 Introduction to Wavelets

Wavelets are small waves that decay to zero with time. The traditional sinusoidal functions used for the Fourier series cannot be considered as wavelets because they have non-zero magnitude for all time. Mathematically wavelets can be defined as having finite energy, or the integral of the squared function must be finite, and also having a null average, or the area under the curve must be zero. This can be expressed as follows:

$$\int_{-\infty}^{+\infty} |g(x)|^2 \, dx < \infty \qquad (1)$$

$$\int_{-\infty}^{+\infty} g(x) dx < 0 \qquad (2)$$

where $g(x)$, a complex function, represents a wavelet. There are other properties that wavelets can be required to possess. One of the most important of these is orthogonality. Although not always

required orthogonality ensures uniqueness of representation in waveform identification and storage and is a must when investigating solutions to Ordinary Differential Equations. Other properties which are attractive but not required are differentiability, which ensures a smooth function, and compact support, which ensures that the wavelet is identically zero outside a certain range [8].

Some of the examples of wavelets are shown in Figure 1. The first wavelet, the Haar wavelet, is the simplest and earliest wavelet documented. It obeys all of the criteria discussed above except differentiability, i.e. it is not smooth. This implies that choosing a suitable set of Haar wavelets to represent a smooth waveform becomes difficult and not economical. Other examples of wavelets are the Daubechies, The Coiflet, and the Syrnmlet. The Daubechies wavelet has rigorous mathematical support and has served in many applications outside the power systems area, such as signal and image processing. The wavelets in Figure 5 were generated using WaveLab, software that is publicly available on the Internet from Stanford University [10]. Wavelab was written in Matlab and uses filter bank theory to generate most of the wavelet waveforms.

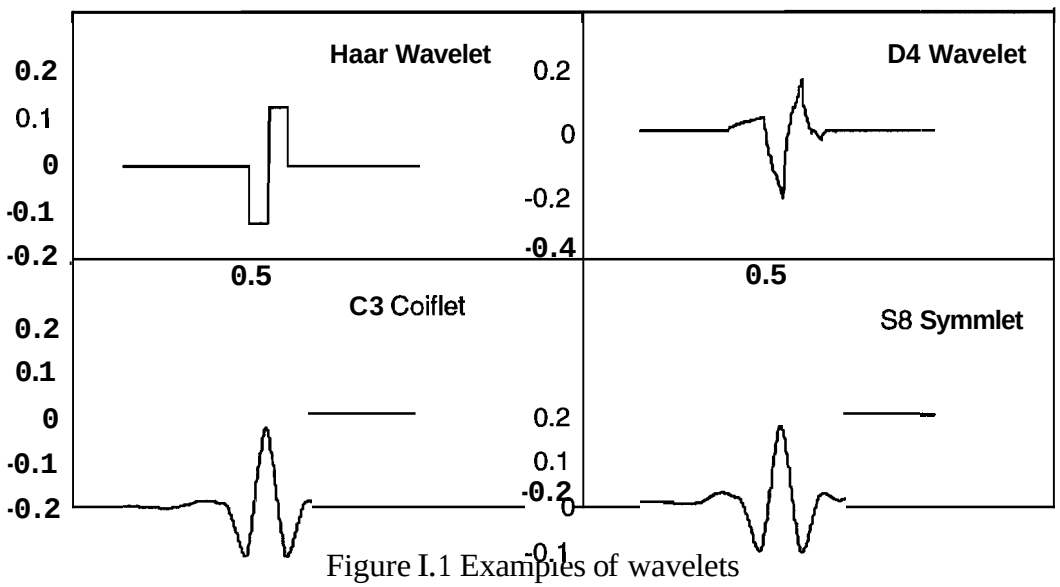

Figure I.1 Examples of wavelets

Another example is the Morlet wavelet shown in Figure 2. This was used as the "mother" wavelet for the Discrete Wavelet Transform in the comparison with the Discrete Fourier Transform to be discussed later. The Morlet wavelet has the following simple mathematical representation:

$$g(t) = e^{-\alpha t^2 + j\omega t} \qquad (3)$$

where α controls the decay rate of the wavelet towards zero and ω controls the frequency. Note the similarity with the Fourier functions if alpha is zero. The mother wavelet refers to the example function **(3)** based on which a set of member functions is generated. The family, or set of functions is built by dilating, or translating the mother wavelet. This family is expressed as:

$$g_{a,b}(t) = g\left(\frac{t-b}{a}\right) \qquad (4)$$

where a controls the dilation of the wavelet and b the translation. Figure 2 shows a Morlet mother wavelet and its family members. If a and b are taken as continuous numbers, the wavelet transform produces redundant information. To avoid this problem, a and b are usually taken as discrete numbers that vary logarithmically with a base of 2. This will be discussed further in the next section.

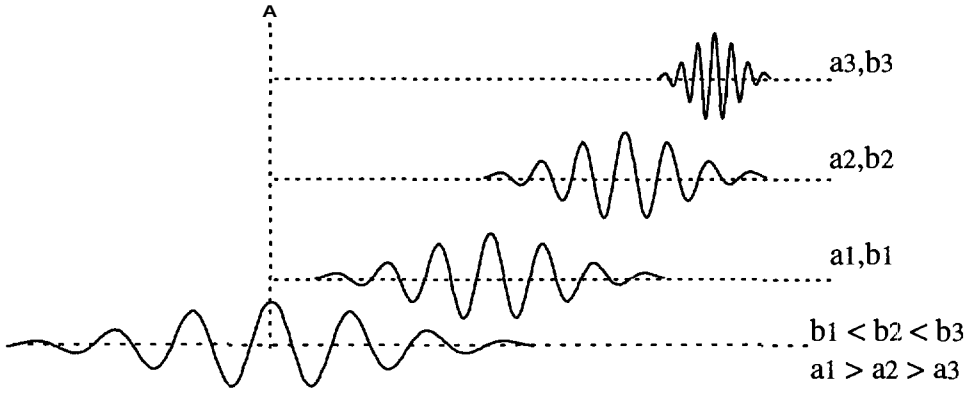

Figure 1.2 A Morlet mother wavelet and members of its family.

1.3 Wavelet Transform

The wavelet transform maps a time domain function into a function whose dependent variables are translation and dilation with respect to the mother wavelet. While the Fourier Transform can be plotted on a 2 dimensional plot whose axes are frequency and magnitude (or phase), the Wavelet Transform requires a three dimensional plot whose horizontal axes represent dilation and translation and the vertical axis may represent magnitude (or phase). The Integral Wavelet Transform is expressed as follows:

$$F_{a,b} = |a|^{-\frac{1}{2}} \int_{-\infty}^{\infty} f(t) g^* \left(\frac{t-b}{a} \right) dt \qquad (5)$$

where the constant in front of the integral is for normalization. In order to avoid the redundancy that results from using a continuous set of values for *a* and b, these are usually taken as follows:

$$\begin{aligned} a &= a_o{}^m \\ b &= k a_o{}^m \end{aligned} \qquad (6)$$

The Wavelet Transform then becomes:

$$F_{m,k} = \left| a_o{}^m \right|^{-\frac{1}{2}} \int_{-\infty}^{\infty} f(t) g^* \left(a_o{}^{-m} t - k \right) dt \qquad (7)$$

where m and k are taken as discrete numbers. As m increases, the wavelets dilate and as k increases the wavelets are translated farther away from the origin. When a_o is taken as 2, we have what is referred to as dyadic translation and binary dilation. In an analogous fashion the Discrete Wavelet Transform is written in terms of the discrete time n as:

$$F_{m,k} = \left| a_o{}^m \right|^{-\frac{1}{2}} \sum_{n} f(n) g^* \left(a_o{}^{-m} n - k \right) \qquad (8)$$

The above summation can be thought of as the dot product of the discrete function *f(n)* and the conjugate of the wavelet *g(m,k)*. As an example of a Wavelet Transform plot, a sinusoid containing two discrete frequencies was used as an input to the Morlet Wavelet Transform. The resulting three dimensional plot is shown below. The transform was done using Matlab.

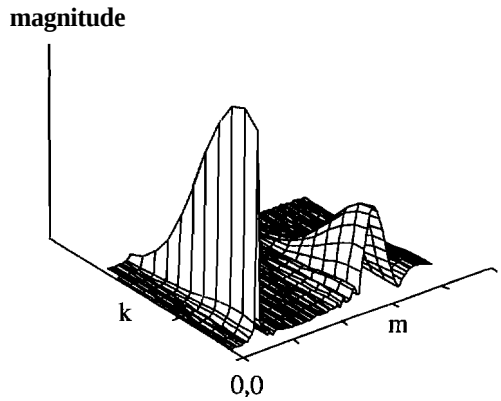

Figure **1.3** Example of a Wavelet Transform magnitude vs. dilation and translation for a waveform containing two discrete frequencies

1.4 Comparison with Fourier

Power system transients are often of a broadband nature. For example, an SVC may cause, upon switching, frequencies around a kHz that superimpose on the 60 Hz fundamental. In order to accurately identify this transient, we could look at the spectrum of the data record. An accurate spectrum needs to resolve both the 60 Hz and the high frequencies. The discussion that follows shows why this a difficult task for a Fourier analysis but readily feasible in terms of the Wavelet Transform.

One of the most restrictive factors that comes with any useful application of the Fourier Transform is the periodicity condition that the input function or the data record has to assume. In fact, if the input function is not periodic, we need the infinite past history as well as the infinite

future history to determine the spectral information of the input function using the Fourier Transform [8]. **A** way around this is to assume periodicity for the length of the data record. The result is an increase in the sidebands of the frequencies of interest because the input function or data record becomes the unintended product of a square window function and the input data record. In order to limit the increase of the sidebands, windowing techniques, such as Hamming, Hanning, and the Short Time Fourier Transform (Gibbons Transform) were developed. This resulted in an improvement for the frequency of interest but not for all the frequencies present in, for example, a broadband signal. **A** broadband signal requires a window that is long for low frequencies and short for high frequencies. This is exactly what the Wavelet Transform provides. If the mother wavelet is chosen appropriately, the low frequencies are analyzed with wavelets that are dilated in shape, and the high frequencies are analyzed using ,wavelets that are compressed in shape. Before we move on to a numerical example, it is worth noting one more difference between Fourier and wavelet analysis. If a and b are taken discretely as shown in (7) then the coefficients that result are the same as the coefficients that are used to represent the input function in terms of wavelet series as follows:

$$f(t) = \sum_{m,k=-\infty}^{\infty} c_{m,k}\, g_{m,k}(t),$$

$$c_{m,k} = F_{m,k} \qquad (10)$$

where the F coefficients are a direct result of the Integral Wavelet Transform in (7). This relationship between transform and series is not possible with the Fourier analysis. This allows Wavelets to be an efficient medium of storage for nonperiodic functions. It was shown by Rebiero (11) that a square pulse may be represented by as few as 5 wavelets while it takes about

32 harmonics to reach the same accuracy. The following numerical example illustrates the above discussion, first in terms of a broadband steady state input datarecord, then a characteristic transient, found in capacitive switching.

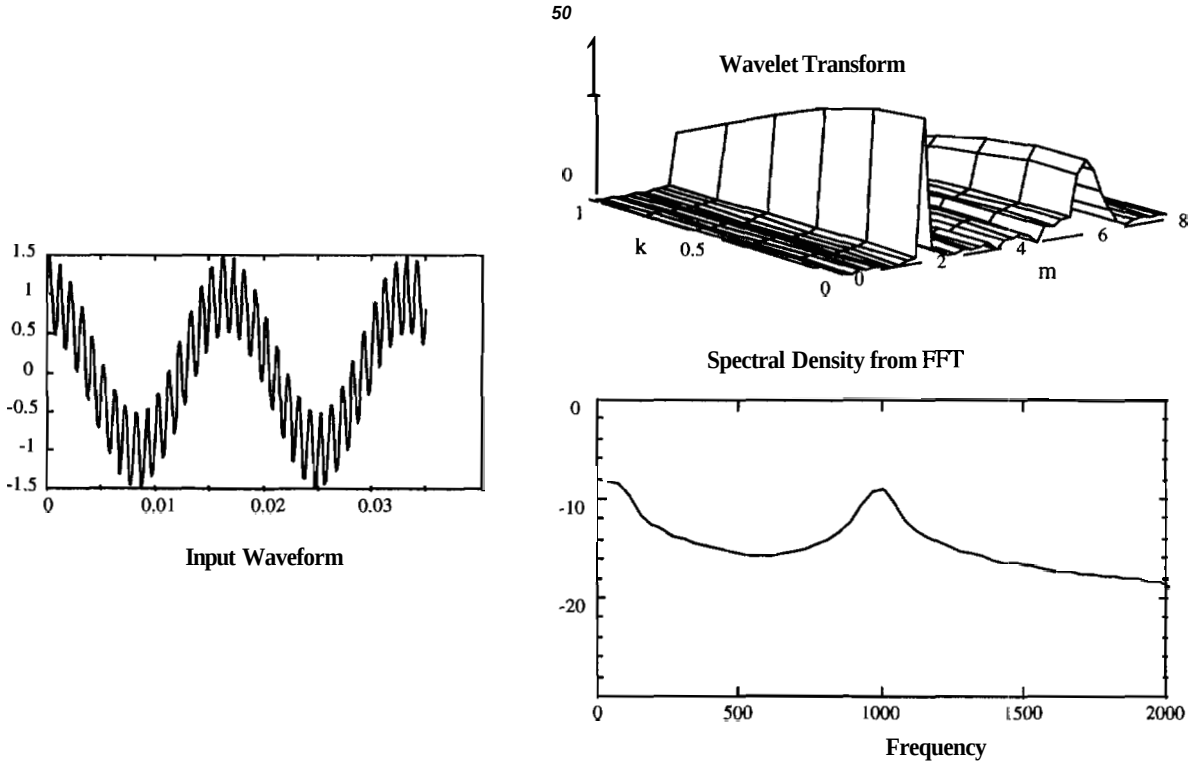

Figure 1.4 Fourier and Wavelet Transform output of a Broadband signal

In Figure 4 a 1 kHz steady state signal is superimposed on a 60 Hz fundamental. The resulting waveform is used as an input function for the DWT and the DFFT. In this example, the ***spectrum*** command in Matlab was used to accomplish the FFT, While the Wavelet Transform was accomplished using a Morlet mother wavelet implemented in a short Matlab file that is given in the appendix. The results from the FFT show that there are two prominent peaks, but it is difficult to determine where the lower frequency actually occurs. There is a smearing effect due to the sidebands and to the windowing techniques that are automatically used in any software

package (in this case Matlab). The Wavelet Transform also shows two prominent peaks. In this case however, the two peaks are easily identifiable. Note that there is a direct relationship between dilation factors and the frequencies of the wavelets. In the next example, we examine similar results for a transient case.

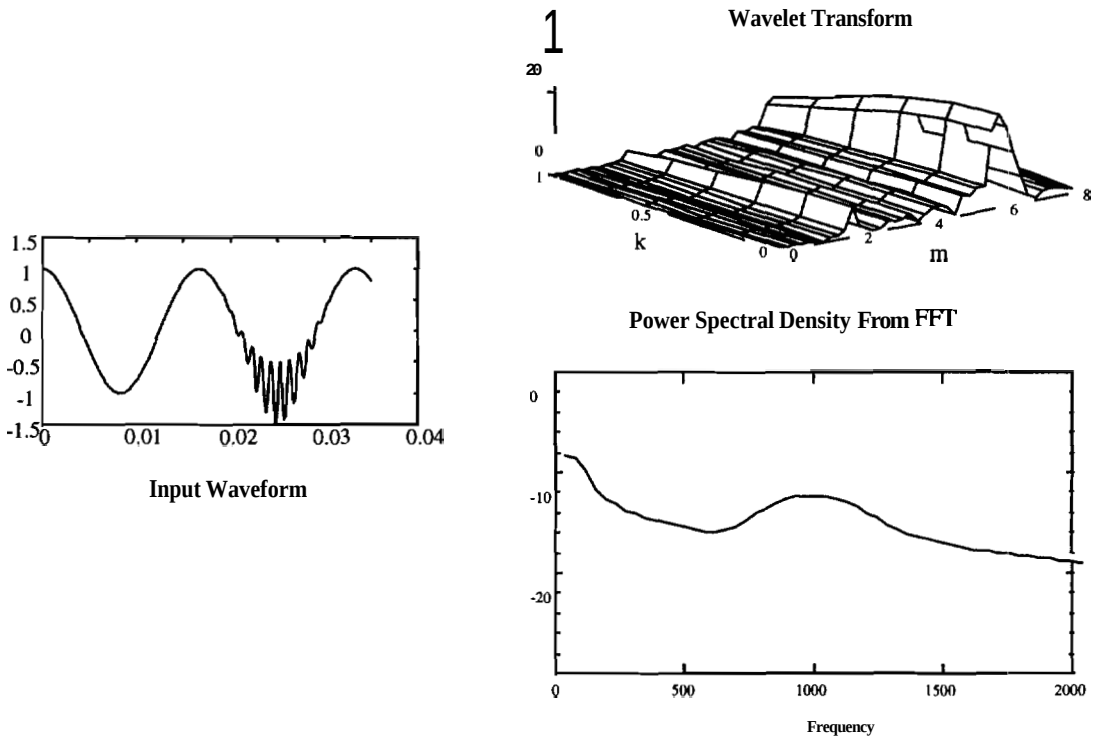

Figure 1.5 Fourier and Wavelet Transform of a high frequency transient on the fundamental

To simulate high frequency transients on power lines, such as those due to solid state switching, or capacitive switching, a one kHz decaying sinusoid was superimposed on the fundamental as shown in Figure 5. The spectrum from the FFT is now very difficult to use in accurately identifying the frequencies present in the input waveform. The sidebands present around one kHz are high enough to produce considerable error. The frequency of the fundamental is not obvious either. The Wavelet transform however, still produces two prominent peaks. Although the high

frequency peak (low m) is lower, due to decaying transient in the input waveform, the associated peak in the DWT is clear enough to determine the frequency. The above examples illustrate briefly the DWT capability in accurately identifying transients. The next section will discuss more general applications for power system transients.

1.5 Applications For Power System Transients

Some of the applications for wavelets in power systems are identification, storage, and analysis of transients. As was shown in the previous section, Wavelet Transforms can be used in identification of transients more accurately than Fourier analysis. Once a transient is identified, it can be efficiently stored using similar techniques. This will allow easy classification of transients and the source of the disturbances. Transient categories such as high and low impedance faults, capacitor switching, transformer inrush current, large motor starts, voltage flicker, and nonsimultaneous pole closure can be easily formed. Then a decision can be made on which transients to keep and which to discard. A recognition system [9] can be trained to detect incipient modes of failure in transformer windings or other on-line equipment. Also, identification of the source cause of transients can aid in resolving power quality conflicts in utility-industrial interfaces. Analysis of transients and propagation in power systems is one of the most recently proposed applications for wavelets [5]. The attempt in this area is to reduce transient analysis to an analysis similar to the harmonic analysis. Harmonic analysis decomposes the forcing current (or voltage) into harmonics which can be used in conventional circuit theory. The result is then obtained from the superposition of the effects of the individual harmonics. In a similar manner, a forcing transient current (or voltage), as in lightening surges, could be decomposed into wavelets with suitable characteristics. The effect of the transient current

(voltage) can then be obtained from the superposition of the effects of the individual wavelets. To extend the analogy further, in harmonic analysis the time domain system model is mapped into a frequency domain model. Likewise, in wavelet analysis of transients, the time domain of the system model will have to be mapped into a dilation-translation model, i.e. each system element will have an equivalent wavelet impedance. The choice of an appropriate set of wavelets will preferably represent the largest possible number of different classes of power transients and result in convenient wavelet impedances that lend themselves to conventional circuit analysis. At this stage a full analysis including the above properties has not been realized yet.

1.6 Conclusion

In the past ten years, wavelet theory and applications have made great strides in fields outside the power engineering area, such as signal and image processing. It is only in the past couple years that wavelet analysis has been introduced for power system transients. The effort in this area has been very recent and seems to be moving in two main directions. One is concerned with the accurate identification and classification of transients. The other is more concerned with the development of an analysis tool to study the effects of transients on power systems.

1.7 References

[1] Amara Graps, " An Introduction to Wavelets," E E E Computational Science and Engineering, Summer 1995, vol. 2, num. 2.

[2] Stephane G. Mallat, " A theory for Multiresolution Signal Processing: The Wavelet Representation," E E E Transaction on Pattern Analysis and Machine Intelligence. Vol. II. NO. 7. July 1989.

[3] Y. Meyer, "Wavelets: Algorithms and Applications," Society of Industrial and Applied Mathematics, Philadelphia 1993, pp. 13-31,101-105.

[4] I. Daubechies, "Orthogonal Bases of Compactly Supported Wavelets," Comm. Pure Appl. Math., Vol. 42,1988, pp. 906-966.

[5] G. T. Heydt, A. W. Galli, "Comments on Power Quality Assessment Using Wavelets," Center for Advanced Control of Energy and Power Systems, Purdue University, W. Lafayette, IN 47905-1285.

[6] Paulo F. Ribiero, " Wavelet Transform: an Advanced Tool For Analyzing Non-Stationary Harmonic Distortions in Power Systems," proceedings IEEE ICHPS VI. Bologna, Italy. Sept. 21-23,1994. pp. 365-369.

[7] David C. Robertson, Octavia I. Camps, Jeffrey S. Mayer, and William El. Gish, "Wavelets and Electromagnetic Power System Transients," GS-SPM95-02. 1995 IEEE Power Engineering Society Summer Meeting, Portlan, Oregon.

[8] Charles K. Chui, An Introduction to Wavelets, Academic Press, Inc., San Diego, 1992.

[9] David C. Robertson, Octavia I. Camps, Jeffrey S. Mayer, "Wavelets and power system transients: feature detection and classification" GS-SPM95-02. 1995 IEEE Power Engineering Society Summer Meeting, Portlan, Oregon.

[10] **http:llplayfair.stabford.edu/"-wavelab(** Wavelab Matlab Software)

18 Appendix

```
step =1.e-4;n=0:step:0.035;a=2;          % Initialize time n and take a=2.
% Generate input function with 60 Hz fund and decaying exponential as transient
f=cos(120*pi*n)+0.5*sin(2000*pi*n).*exp(-100000*(n-0.025).*(n-0.025));
plot(n,f)
pause
i=1;j=1;
%Generate m and k
m=0:0.2:8;mi=length(m);
am=a.^m;                                 % Calaculate a^m
k=0:0.2:1;ki=length(k);
F=zeros(ki,mi);                          % Initialize F
for i=1:ki;                              % Start double do loop
for j=1:mi;
T=(n-k(i)*am(j))/am(j);                  % Genarate time vector for wavelet
g=exp(-1.*T.*T).*exp(8000*pi*T*sqrt(-1)); % Generate wavelet
F(i,j)=f*conj(g')/sqrt(am(j));           % Generate DWT in terms of inner product off and g
end
end
subplot(211)                             % Genrate 3D plot for F
mesh(m,k,abs(F))
subplot(212)
FF=spectrum(f);                          % Fenerate FFT off
specplot(FF,1/step)
axis([0 2000 1.e-20 1.e10])
```

Chapter II
Voltage Flicker
Jamie Edwards

71.1 Introduction

In recent years concern about flicker on power systems has increased, perhaps due to the increasing number of flicker-producing loads connected to the power system. One major source of flicker is the electric arc furnaces used at steel production facilities. An increasing percentage of steel mills, including the aggressive mini-mills, are using electric arc furnaces[1]. The popularity of DC furnaces has also contributed to the evaluation of their effects on power systems compared to traditional AC furnaces. Electric utilities are faced with the challenge of providing high quality power to all customers as well as high short circuit capabilities to minimize the effects of large arc furnace loads. One main concern in operating an arc furnace, which is a rapidly varying load, is voltage flicker on the power system. In the planning stage, various methods are utilized to estimate the capacity of the power system required to operate the furnace and avoid voltage flicker problems. As a general rule of thumb, the ratio of the arc furnace MVA to the utility available short circuit MVA can yield some insight into the likelihood of potential problems. In general, the higher the ratio the better, but a ratio of 80 or larger is sometimes used as a guideline to determine if serious study efforts are required.[2]

71.2 Definition of Voltage Flicker

Voltage flicker is the amplitude modulation of the fundamental frequency voltage waveform by one or more frequencies, typically in the 0 to 30 Hz range. This modulation

causes a periodic brightening and dimming of lights connected to the modulated voltage, hence the term flicker. Voltage flicker is expressed as the RMS value of the modulating waveform divided by the RMS value of the fundamental waveform. This is equivalent to expressing voltage flicker as the change in voltage divided by the voltage. Flicker is usually expressed as a percentage (%dV/V).

The New IEEE Standard Dictionary of Electrical and Electronics Terms defines flicker in the following way:

> **flicker(1)** (television). **(A)** (general). Impression of fluctuating brightness or color, occurring when the frequency of the observed variation lies between a few hertz and the fusion frequencies of the images.

When exposed to the same voltage modulation, different types of lighting may produce different variations in output light intensity. For this reason the terms *voltage flicker* and lightflicker (or lampflicker) are not interchangeable. The scaling difference between the voltage flicker and the light flicker for a given light has been called the *gain* factor for that type of light. When the term *flicker* is used alone in a power engineering context it is most commonly referring to voltage flicker.

Some organizations have defined flicker as the peak-to-peak value of the modulating waveform divided by the peak value of the fundamental waveform. This definition will produce flicker values that are double those obtained using the conventional definition. There is nothing inherently wrong with such a definition as long as the flicker limit curves are adjusted to match this definition. The definition of flicker can be checked by generating flicker in a laboratory and comparing it to both the commonly accepted flicker curves and human observation. When this is done, light

flicker becomes perceptible just as the flicker values exceed the limit curves, when the **RMS** value of the modulating waveform divided by the **RMS** value of fundamental waveform definition of flicker is used.[1]

II.3 Possible Flicker Waveform

Figure II.1 shows a 60 Hz waveform with 5% at 10 Hz. The modulating waveform is also shown. Figure II.1 shows only one flicker frequency with a very high magnitude. In most cases it is not possible to visually identify the multiple flicker frequencies and corresponding magnitudes present in a voltage waveform. The human eye is most sensitive to flicker (modulation) frequencies in the 6 to 10 Hz range. Flicker levels of 0.3% to 0.4% are visible in this frequency range. The human eye is progressively less sensitive to frequencies below this range. This is why it is important to measure both the magnitude and the frequency of any modulation of the voltage waveform.

In actual power system voltage waveforms, multiple flicker modulation frequencies are present. The flicker produced by these multiple frequency components can be calculated by means of analog or digital filtering techniques or by means of a Fast Fourier Transform (FFT) algorithm. An advantage of performing an FFT is the fact that the frequency spectrum information is easily obtained. This is useful information for analyzing a flicker problem or the effects of flicker reduction equipment such as static var compensators or furnace electrode position control systems.[1]

II.4 Common Causes of Flicker

Flicker phenomena can be divided into two general categories, cyclical flicker and non-cyclical flicker. Cyclical flicker is caused by fluctuating loads such as electric arc furnaces, arc welders, and reciprocating pumps and compressors. Non-cyclic flicker is caused occasional load fluctuations such as may be caused by the starting of a large motor. The load fluctuations must be quite large to cause flicker on a power system. Common household appliances may cause flicker in one persons house, but does not normally cause a large enough variation in load current to affect the neighbors.[2]

Flicker is closely related to the short circuit MVA of the source and the MVA size of the load. For a fixed load size, a strong, or stiff, source (high short circuit MVA) will tend to reduce voltage flicker as compared to a weak source. This is due to the fact that flicker is caused by variations in load current and the voltage drop across the source impedance caused by the load current. When the load current varies, the voltage throughout the system will vary as well. A stiff source means a lower source impedance which means less voltage drop for a given change in load current.

Loads which do not usually cause flicker may be a source of background flicker on a power system. The flicker generated by these loads is of a very low level and is predominantly in the low frequency regions of a flicker spectrum. This can be explained by changes in load. Whenever a large load is disconnected or connected the voltage will rise or fall slightly, respectively. A flicker meter will sense these voltage changes and report flicker in the low frequency range. This is consistent with observation. If a large load is started people notice the light intensity drop for a moment. This low frequency

flicker will be present a very small percentage of the time and is an example of non-cyclical flicker.[1]

II.5 Calculation of Flicker and Flicker Standards

The mathematical relationships and definitions of voltage flicker used in this paper are described in Figure II.1 with a sample voltage waveform with a cyclical modulating envelope.

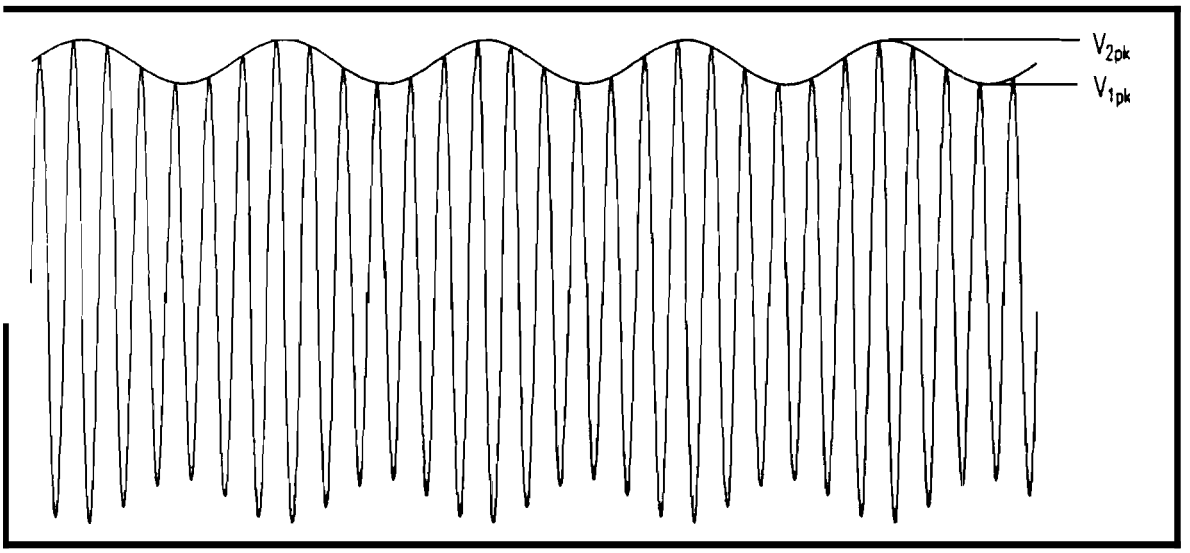

$$\textit{Where,} \qquad \Delta V = V_{2pk} - V_{1pk}$$

$$'mod\ \ ulating\text{-}RMS - \frac{\Delta V}{2\sqrt{2}} - \frac{V_{2pk} - V_{1pk}}{2\sqrt{2}}$$

$$Average\ V_{fundamental-RMS} = \frac{V_{2pk}/\sqrt{2}}{2} + \frac{V_{1pk}/\sqrt{2}}{2} = \frac{V_{2pk} + V_{1pk}}{2\sqrt{2}}$$

$$Percent\ Voltage\ Flicker(\%dV/V) = \frac{V_{2pk} - V_{1pk}}{V_{2pk} + V_{1pk}} * 100\%$$

Figure II.1 Sample voltage flicker waveform and mathematical relationships[2]

There are no established industry standards defining acceptable flicker levels; but, a variety of perceptible flicker curves (flicker limit curves) are available in published literature, which can be used as guidelines to verify whether the amount of .voltageflicker is a problem. The establishment of a tolerance threshold is subjective, since it is influenced by many variables. Factors affecting the determination of a limit for flicker can include ambient lighting levels, size and type of lamp, room decor, duration, and the abruptness of the voltage variation, and the intensity and immediate occupation or interest of the observer. EEE Standard 519-1992, EEE Recommended Practices and Requirements for Harmonic Control in Electrical Power Systems, and ANSI/IEEE Standard 141-1986, IEEE Recommended Practice for Electric Power Distribution for Industrial Plants are documents in which data from various sources for perceptible flicker can be found.[2]

II.6 Flicker Limit Curves

Although the eye is sensitive to changes in light intensity, it is common to speak of perceptible flicker levels in terms of the voltage fluctuations that cause the variations in light intensity. Incandescent light bulbs produce a slightly higher change in light intensity for a given amount of voltage flicker than do most fluorescent bulbs. For this reason most flicker curves are based on how much voltage flicker causes a majority of viewers to observe light flicker from an incandescent bulb.

Curves have been developed to express the magnitude and frequency of flicker that is visible to the human eye. Because there are so many variables in the perception of flicker, many flicker curves have been developed to represent visible flicker. No two

pairs of human eyes are identical so some researchers have plotted families of curves: one curve where 10% of the observers see flicker, another curve where 20% of the observers see flicker, and so on.

Some researchers distinguish between perceptible flicker and objectionable flicker levels. For the purposes of analysis, however, the perceptible flicker curves are used as a more conservative way to evaluate the effects of voltage flicker. Using a perceptible flicker curve should keep the flicker levels below the objectionable level. Unlike harmonics, which cause well-known problems in a power system, the final determination of whether there is a flicker problem is whether the utility receives complaints from customers who observe flicker.[1] One possible flicker limit curve is shown in Figure 2.1 below.

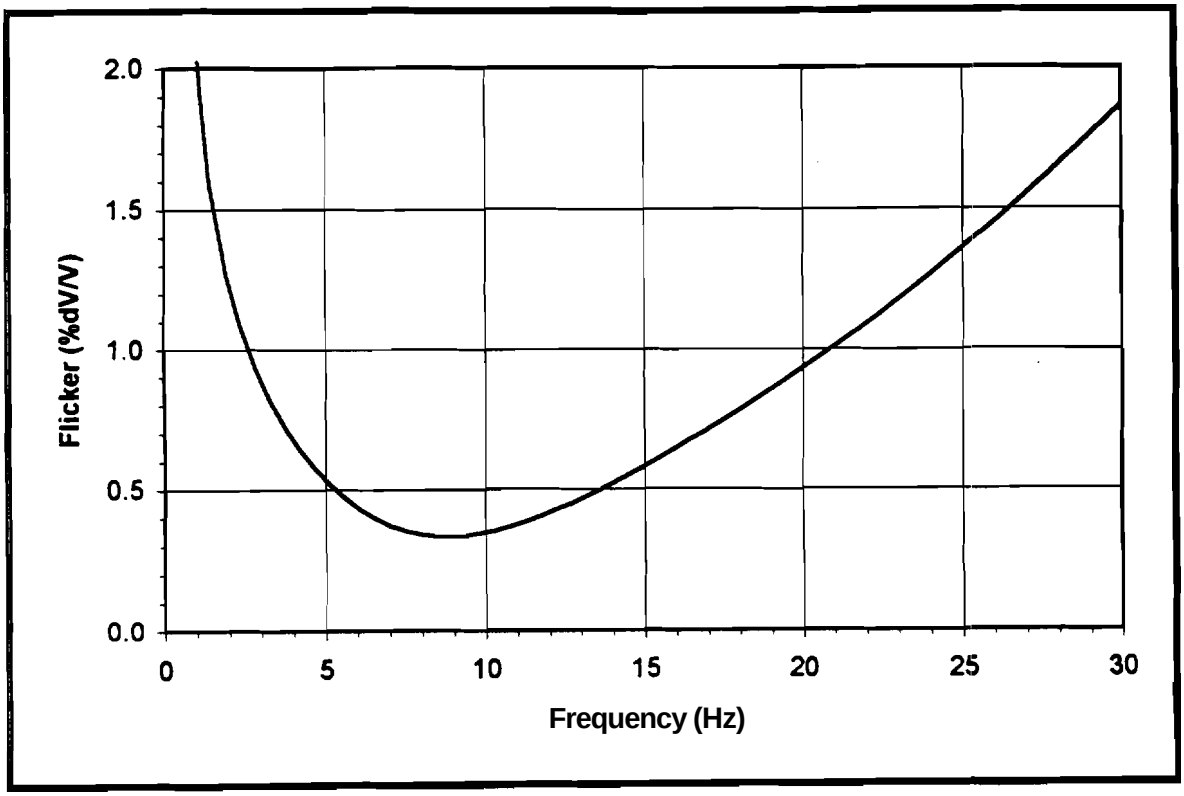

Figure II.1 Possible flicker limit curve.[1]

The previous section mentions the best sources for flicker guidelines and standards.

II.7 Corrective Measures and Conclusions

Operation of rapidly varying loads such as AC and DC arc furnaces in large industrial power systems will cause voltage flicker on the utility system. System planning can help in determining the available short circuit duty at a point of common coupling between the flicker load and system to keep the voltage flicker within acceptable limits. Perceptible flicker limit curves are useful in determining the amount of flicker in a system. When applicable, on-site field tests with equipment that will accurately capture multiple frequencies can aid in measuring the existing voltage flicker. At that point a determination can be made whether the problem is severe enough to further study or pursue corrective measures to remedy the problem.

Some common corrective measures that are effective in providing economical reactive power support for electric furnace supply systems are: capacitor banks and/or harmonic filters. Power factor penalties and demand charges can also be reduced or eliminated. The design of the power factor correction system must be carefully engineered so as not to itself create voltage flicker problems themselves. Harmonic analysis studies are helpful to insure a proper system design. Field measurements are desirable to eliminate the number of assumptions that are required in performing the studies. The ultimate determination whether acceptable voltage flicker exists in a system will be complaints from customers served by the utility system actually experiencing objectionable or noticeable flicker.[3]

Bibliography

Publications and references used for this report include:

[1] Blooming, Thomas M.. "Relating Flicker Limit Curves to Visible Flicker" Cooper Power Systems System Engineering Reference Bulletin SE9502 August 1995: 1-27.

[2] M.T. Bishop, A.V. Do, and S.R. Mendis. "Voltage Flicker Measurement and Analysis System" IEEE Computer Applications in Power 1994: 34-38.

[3] S.R. Mendis, M.T. Bishop, and J.F. Witte. "Investigations of Voltage Flicker in Electric Arc Furnace Power Systems" IEEE/IAS 29th Annual Meeting October 1994: 1-8.

Chapter III

Transients in Electric Power Systems due to Shunt Capacitor Switching

Naeb-boon Hoonchareon

III.1 Introduction

Shunt capacitors are used extensively in power transmission and distribution systems as a mean of supplying reactive power. The main advantages of using shunt capacitors are their low cost and their flexibility of installation and operation. These capacitors are implemented in the system in order to control system voltage, to increase power transfer capability, to reduce equipment loading, and to reduce energy costs by improving power factor of the system. It can be said that by far the most economic means of providing reactive power and voltage support is the use of shunt capacitors[1].

However, energizing these shunt capacitors produces a transient oscillation in the power systems. Due to the fact that the operation of switching shunt capacitors happens frequently, shunt capacitor switching is regarded as the main source of generating transient voltages on many utility systems. These transients can cause damages on both utility systems and customer systems, depending on the system parameters such as switched shunt capacitor size, transformer size, and the type of customer loads connected to the system.

In this paper, transient characteristics resulting from shunt capacitor switching are studied, impacts of varying system parameters on transient voltages are examined, and methods used to control transient overvoltages are discussed. The case study used for the analysis of

changing system parameters and the illustrations of simulation results presented here are excerpted from the reference paper[2].

111.2 Transient characteristics of three phase shunt capacitor switching

The single line diagram of the power system shown in Fig.III.1 will be used to analyze transient characteristics due to shunt capacitor switching.

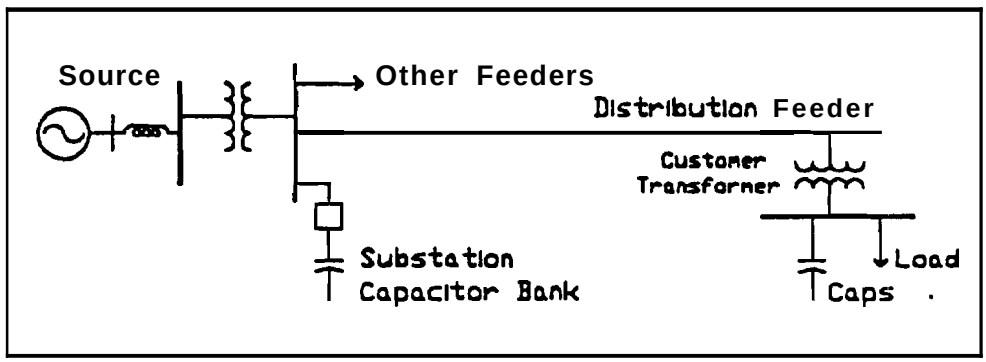

Figure III.1 Single line diagram for example power system.

To simplify the ideas, the system is divided into two parts of different LC circuits as shown in Fig.III.2. The circuit in part one consists of L1 and C1, which can be viewed as system inductance(from source and step-up transformer) and switched shunt capacitance, respectively. Likewise, the circuit in part two consists of L2 and C2, which represents step-down transformer inductance(inductance in distribution lines may also be included) and capacitance appearing at the low voltage bus. The source of the capacitance C2 founded in customer systems can be power factor correction capacitors or capacitors used as a filter in adjustable speed drives.

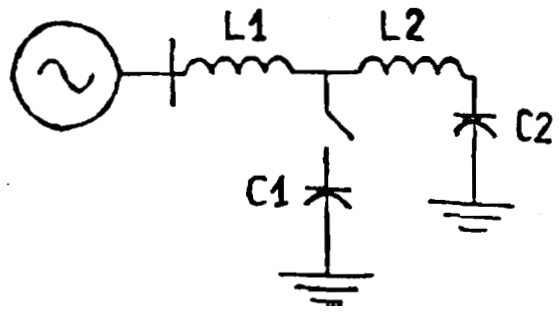

Figure III.2 Simplified equivalent circuit for the example power system.

Energizing a shunt capacitor bank fiom a predominately inductive source can cause an oscillatory transient voltage which can be as high as 2.0 pu at the shunt capacitor location with a resonant frequency o f f = $1/2\pi\sqrt{L1C1}$. The theoretical analysis in detail of shunt capacitor switching has been done in the reference paper[3], using simplified equivalent circuit as shown in Fig.III.3 for the case where shunt capacitor bank is connected in ungrounded-wye. In this equivalent circuit, C_A ,C_B, and Cc represent the shunt capacitor for each phase, **A** B C respectively, while C_N represents the effective capacitance to ground of the bank neutral.

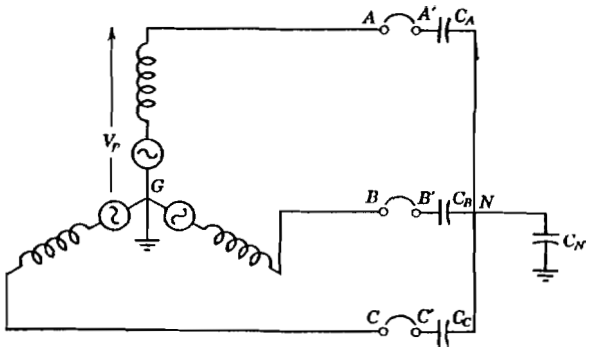

Figure III.3 Simple equivalent circuit for three-phase shunt capacitor switching.

Condition set in this analysis is that at the moment when the switched is opened, phase **A** interrupts first, causing the rest of the system to be a single phase circuit composed of phases B

and C, and then, phases B and C interrupt at the next current zero passing through switching contacts B and C.

Diagram in Fig.III.4 shows the resulting voltages trapped on each capacitor after the switch has been completely opened, which will in turn be initial states for the next switching of shunt capacitor bank back into the system. It is worth noting that the maximum voltage appearing across the switching contacts of circuit breaker at this point can be as high as 2.5 Vp in phase A, $(1+\sqrt{3}/2)$ Vp in phase B, and $(1+\sqrt{3}/2)$ Vp in phase C. These voltages may induce restrikes or reignitions in the circuit breaker, which in turn can lead to much higher transient voltages that can result in serious damages on the utility system. For further analysis of transients due to restrikes, we refer the reader to the reference paper[3].

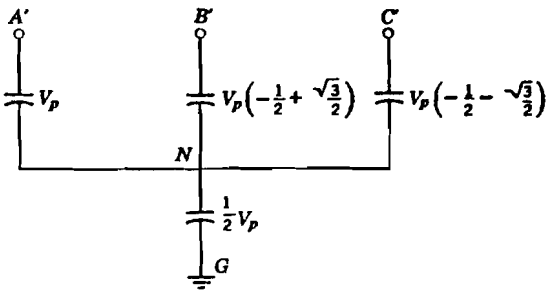

Figure III.4 Voltage trapped on the capacitor after the switch is opened.

Transients due to shunt capacitor switching in the LC circuit in part one(L1 and C1) can excite an LC circuit in part two(L2 and C2), resulting in transient magnification at the low voltage bus where C2 is connected. This happens when the resonant frequencies of these two LC circuits are in the same range. The worst case magnification occurs when the ,following conditions are satisfied[4]:

1. The resonant frequencies of these two LC circuits are equal; i.e.,

   L1*C1 = L2*C2.

2. The switched shunt capacitor C1 is much larger than the low voltage capacitor C2; i.e.,

   (MVAR C1) >= 25*(MVAR C2).

3. The connected loads at the low voltage bus provide little damping for the system.

To illustrate transient characteristics analyzed above, the case study performed by using Electromagnetic Transients Program(EMTP) and the simulation results from the reference paper[2] are presented here.

According to Fig.III.1, the system conditions for the base case study were set up as follows:

System Source Strength at the Substation = 200 MVA

Switched Shunt Capacitor Size = 3 MVAR

Total Feeder Load = 3 MW

Step Down Transformer Size = 1500 kVA (6% Impedance)

Low Voltage Capacitor Size = 300 kVAR

Customer Resistive Load = 300 kW

Fig.III.5 shows the transient voltage at the switched shunt capacitor, and Fig.LII.6 shows the magnified transient voltage at the low voltage capacitor. Notice that transient voltages in high side are in the range of 1.O-2.0 pu while magnified transient voltages in low side are in the range of 2.0-3.0 pu.

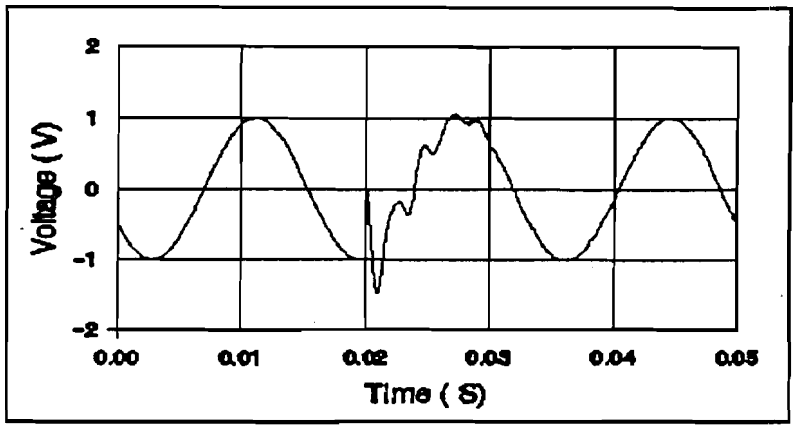

Figure III.5 Transient voltage at the switched shunt capacitor.

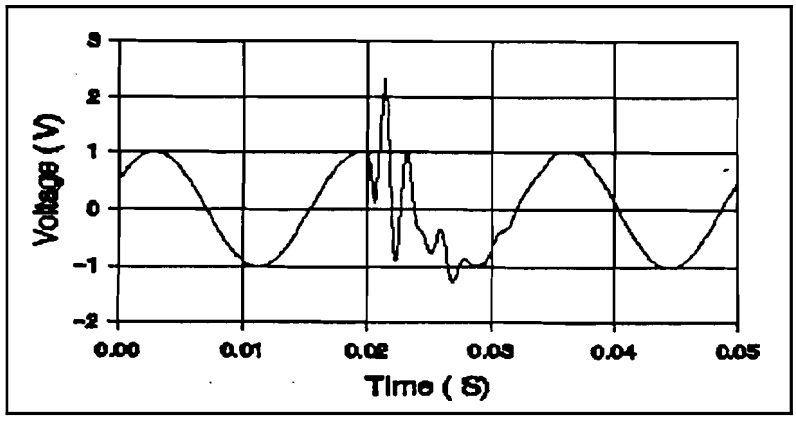

Figure III.6 Magnified transient voltage at the low voltage capacitor.

Practically, the magnitude of these transient voltages is decreased by damping provided by system loads and losses.

111.3 Impacts of varying system parameters on transient magnification

Since magnification occurs when LC circuit in part two can be excited by transient voltages from LC circuit in part one, it can be expected that changing the sizes of switched shunt capacitor, low voltage capacitor, and step down transformer(which is equivalent to changing the system parameters C1,C2, and L2, respectively) can affect the magnified transient voltages. In

system parameters C1, C2, and L2, respectively) can affect the magnified transient voltages. In addition, the characteristics of customer loads at the low voltage bus play an essential part in this magnification, for they provide damping required to reduce the magnitude of transients. The effects of these parameters are illustrated, using the results of the simulation obtained from the reference paper[2].

Fig.III.7 depicts the impacts of switched shunt capacitor size and low voltage capacitor size on the peak transient magnitude in per unit. It's obvious that the higher the differences between the size of switched shunt capacitor and the size of low voltage capacitor, the higher the magnitude of magnified transients. Moreover, as the size of the switched shunt capacitor gets larger, the potential for magnification occurs over a wide range of low voltage capacitor sizes.

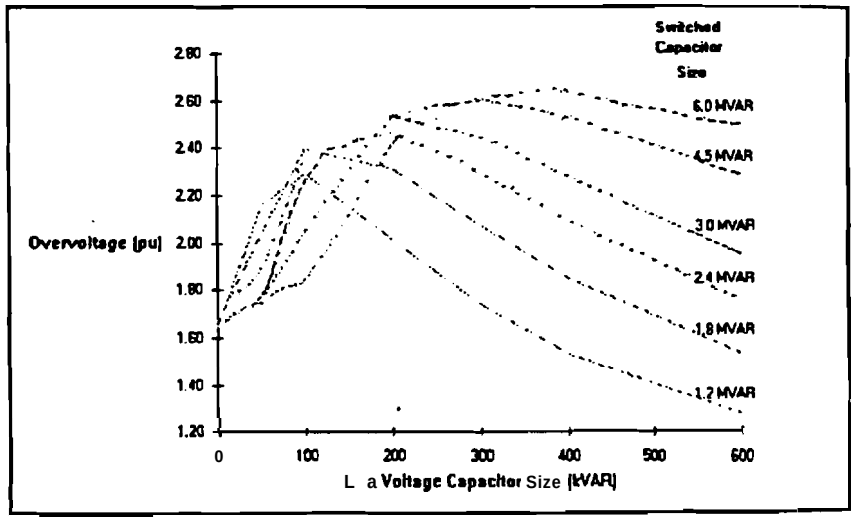

Figure III.7 Transient voltage magnitude at the low voltage bus as a function of switched shunt capacitor and low voltage capacitor sizes.

The peak transient magnitude at the low voltage bus as a function of low voltage capacitor size for three different sizes of step down transformer is shown in Fig.III.8. It can be seen from the curves that the highest magnified transients occurs for higher values of low voltage

capacitor size as the step down transformer size is increased. Furthermore, magnification can occur over a wide range of the low voltage capacitor sizes.

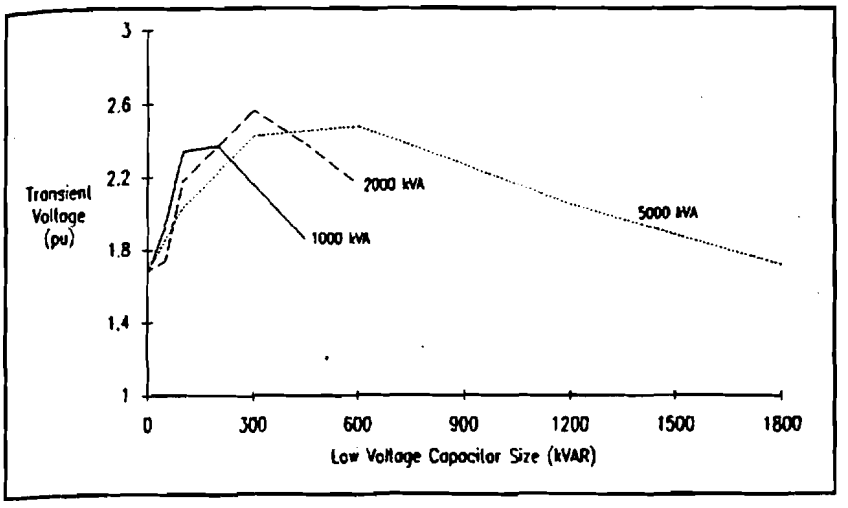

Figure III.8 Transient voltage magnitude at the low voltage bus as a function of the step down transformer size.

Fig.III.9 shows the effect of both resistive and motor load on the magnified transient magnitude, Notified from the curves, resistive load provides good damping while motor load provides only small damping for the system to reduce transient voltages. Unfortunately, it is inevitable for many industrial customers to have their loads dominated by motors.

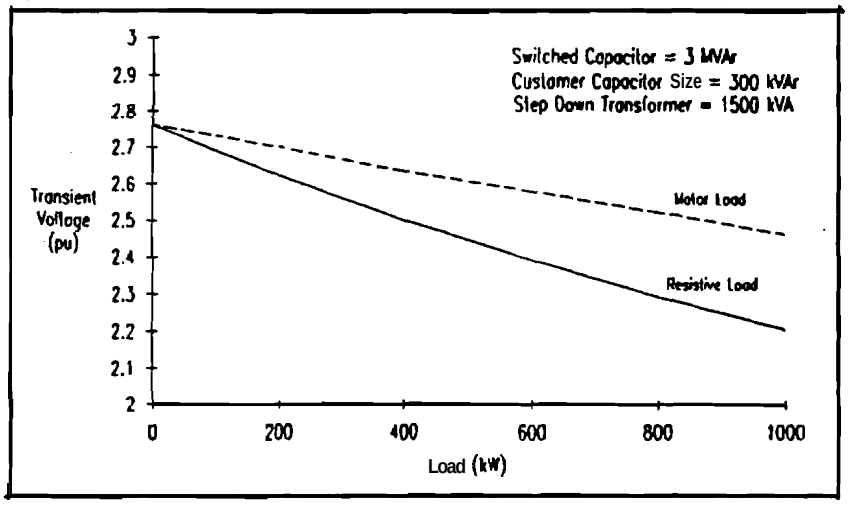

Figure III.9 Transient voltage magnitude at the low voltage bus as a function of customer load characteristics.

Other factors that can affect transient magnification include the source strength at the switched shunt capacitor, the connection of shunt capacitor bank to the system, and the capacitor placement. Basically, the stronger the source(the lower the source impedance), the lower the transient voltages[5]. The study also shows that switched shunt capacitor bank!; connected in ungrounded-wye are likely to produce higher phase-to-phase transient voltages than those produced by switched shunt capacitor banks connected in grounded-wye. Additionally, if the capacitors are more distributed on the distribution feeder, transients can be lowered. The case study done in the reference paper[5] reveals that already energized capacitors on the line tend to reduce transient voltages caused by shunt capacitor switching.

111.4 Transient problems due to shunt capacitor switching

Normally, transient voltages caused by shunt capacitor switching are not a concern for the utility systems because they are below the level at which surge protective devices in the system will operate(l.8 pu or above)[2]. However, in the peculiar conditions when prestrikes or restrikes in the switching device occur, relatively high transients produced by these two conditions can result in severe damages on both the switching device and an overall system.

Prestrike during capacitor energizing can occur when there is an arc forming across switching contacts and contracting before the contacts are completely closed. This arc is extinguished by the switch being able to clear the current zeroes and causing the contacts to close completely. Restrike during deenergizing capacitor can occur when the switch is unable to handle the voltages across the contacts when the switch is opened and therefore, causes the contacts to reclose momentarily. It is essential for utility system suppliers that they use switching devices which have mechanism to minimize the occurrence of both prestrikes and restrikes.

Transients due to shunt capacitor switching may result in failure of transformer. The study shows that energizing a transformer and shunt capacitors at the same time can cause transient voltages that affect the transformer provided that the transients produced have the resonant frequency near one of the harmonics in the transformer inrush current. This will in turn produce substantial overvoltages that last for many cycles at the harmonic frequency. Details of the analysis of capacitor switching and transformer transients are presented in the reference paper[6].

Unlike utility systems, customer systems are significantly affected by transients due to shunt capacitor switching because of magnification that occurs in LC circuit in part two. Usually, magnified transient voltages at the low voltage bus are in the range of 2.0-3.0 pu. These transients have substantial energy that can cause damages on protective devices, electronic equipment, capacitors and other devices connected to the low voltage bus. Some types of power electronic equipment are exclusively sensitive to these transients.

For example, adjustable speed drives(ASDs) are likely to have serious damages when experiencing transients due to shunt capacitor switching even without magnification involved. This is because typically ASDs consists of relatively low peak inverse voltage(PIV) rating semiconductor devices and low energy rating metal oxide varistors(MOVs) used to protect the power electronic equipment[7].

Additionally, customers have encountered the problems of circuit breaker nuisance tripping and the difficulty to coordinate between MOV arresters with relatively high energy used to control transients due to shunt capacitor switching and MOV arresters with relatively low energy used to protect power electronic devices.

III.5 Methods to control transient overvoltages

Methods implemented to solve transient problems due to shunt capacitor switching have been basically derived from the ideas of how to minimize transient voltages and how to eliminate transient magnification at low voltage bus. These methods are as follows[2]:

-Synchronous closing control

This method is to control closing instants of the capacitor switching device so that each phase of the capacitor bank is energized at the time when the voltage across switching contacts is zero. In practice, a vacuum breaker is the only switching device that can be implemented with this concept. It has been proven that synchronous closing control is efficient for large substation banks and transmission system capacitors. This method has not typically been employed for feeder capacitors.

Fig.III.10 shows the impact of the closing instant on transient voltage in LC circuits in both part one and part two.

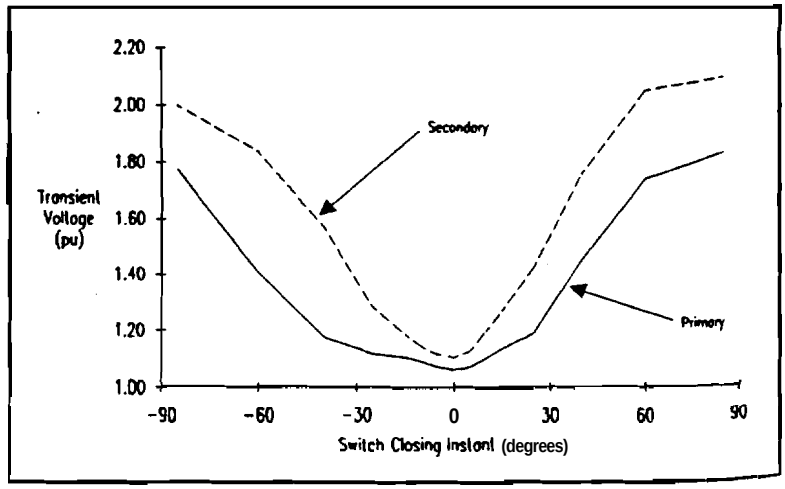

Figure III.10 Transients due to shunt capacitor switching as a function of the switch closing instants.

-Optimum closing/opening resistors

The capacitor switching device may equipped with closing and/or opening resistors optimized to reduce transients caused by capacitor switching, and also to prevent restrikes and prestrikes of the switch. The problem of this method is that normally the optimum size of these resistors are not available for distribution switching devices. Nonetheless, this method is regarded as an effective way in reducing capacitor switching transients in power systems.

Fig.III.11 depicts the effect of resistor size on transient voltage in LC circuits in both part one and part two.

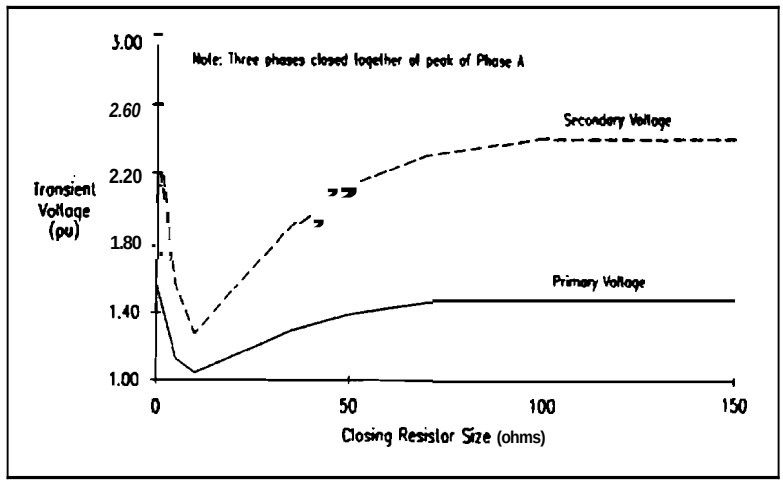

Figure III.11 Transients due to shunt capacitor switching as a function of resistor size used in the capacitor switching device.

-Metal oxide varistor (MOV)

MOV arresters are extensively used in both utility systems and customer systems to reduce transient overvoltages and to protect power electronic equipment. The coordination among these MOVs in the system has to be done properly.

-Harmonic filters

The idea of this method is to eliminate transient magnification by detuning the LC circuit in part two so that its resonant frequency is out of range of the resonant frequency of LC circuit in part one, and hence, not being easily excited by shunt capacitor switching. Fig.III.12 shows the most conventional configuration for low voltage harmonic filters.

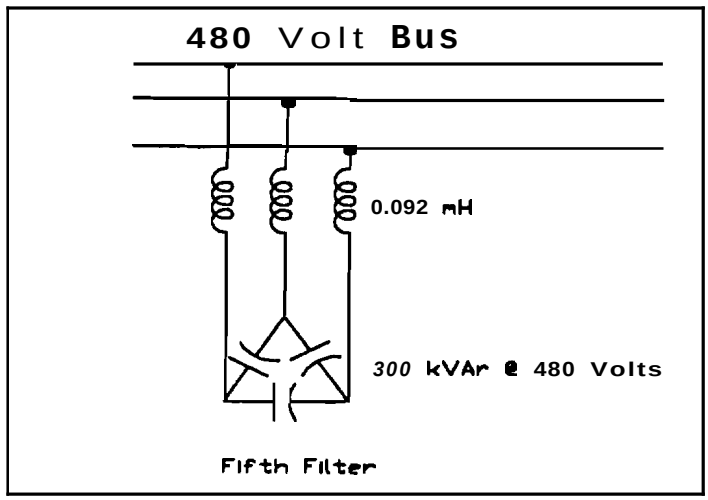

Figure III.I2 Low voltage harmonic filter configuration.

Fig.III.13 illustrates the comparison of transient voltage produced when using harmonic filters as power factor correction with those when using only capacitors. It can be seen from the curves that transient magnification is completely eliminated when applying harmonic filters instead of pure capacitors. However, this method will be effective only if all of the low voltage power factor correction is applied as harmonic filters.

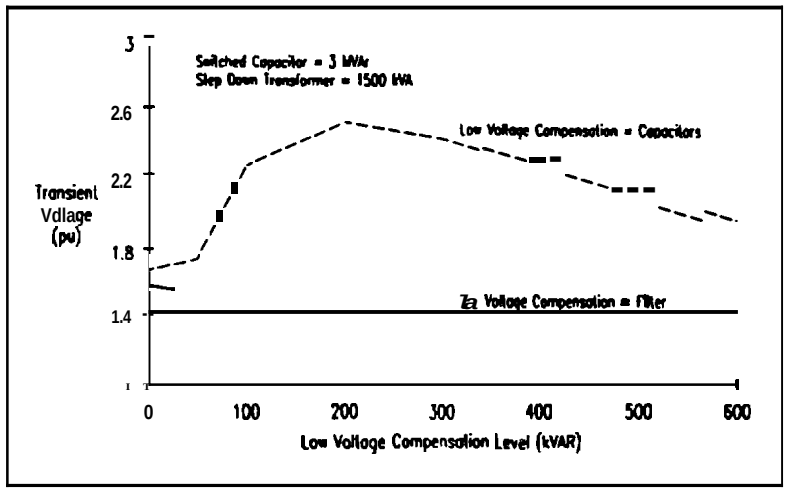

Figure III.13 Transient voltage at the low voltage bus as a function of the type of low voltage compensation.

III.6 Conclusions

Shunt capacitor switching is the main source of generating transients in power systems. These transient voltages can be magnified at the low voltage bus due to inductance-capacitance characteristics formed by customer step down transformer and low voltage capacitors connected to the bus (on the purposes of power factor correction or being a part of electronic circuit load), causing significant interruption and damages on customer systems. The main parameters that have an impact on transients and transient magnification produced by shunt capacitor switching include switched shunt capacitor size, step down transformer size, low voltage capacitor size, and customer load characteristics. The analysis of these parameters gives both utility suppliers and customers an idea of how to solve transient problems which occur in their systems. Methods currently used to control these transient voltages are synchronous closing control on switching devices, optimum closing/opening resistor insertion, the use of metal oxide varistor arresters, and the use of harmonic filters instead of pure capacitor as power factor correction.

References

[1] Kunder, Prabha, Power System Stability and Control, McGraw-Hill Inc., New York, 1994.

[2] M.F. McGranaghan, R.M. Zavadil, G. Hensley, T. Singh, and M. Samotyj, "Impact of Utility Switched Capacitors on Customer Systems-Magnification at Low Voltage Capacitors," IEEE Transactions on Power Delivery, Vol.7, No.2, pp 862-868, April 1992.

[3] Allan Greenwood, Electrical Transients in Power Systems, John Wiley & Sons, Inc., New York, 1971.

[4] A.J. Schultz, J.B. Johnson, and N.R. Schultz, "Magnification of Switching Surges," AIEE Transactions PAS, pp 1418-1426, February 1979.

[5] L.A. Shankland, J.W. Feltes, and J.J. Burke, "The Effect of Switching Surges on 34.5 kv System Design and Equipment," IEEE Transactions on Power Delivery, Vol.5, No.2, pp 1106-1112, April 1990.

[6] R.S. Bayless, J.D. Selman, D.E. Truax, and W.E. Reid, "Capacitor Switching and Transformer Transients," IEEE Transactions on Power Delivery, Vol.3, No.1, pp 34.9-357, January 1988.

[7] M.F. McGranaghan, T.E. Grebe, G. Hensley, T. Singh, and M. Samotyj, "hnpact of Utility Switched Capacitors on Customer Systems, Part II-Adjustable Speed Drive: Concerns," IEEE Transactions on Power Delivery, Vol.6, No.4, pp 1623-1628, October 1991.

[8] M.F. McGranaghan, W.E. Reid, S.W. Law, and D.W. Gresham, "Overvoltage Protection of Shunt Capacitor Banks Using MOV Arresters," IEEE Transactions PAS, Vol.103, No.8, pp 2326-2336, August 1984.

[9] T. Gonen, Electric Power Distribution System Engineering, McGraw- Hill.,1986.

Chapter IV
Electric Arc Furnaces
Omar A. Marte

IV.l Introduction

Electric Arc Furnaces can be regarded as the most disturbing load among today's industrial electrical systems. Their effects can be felt not only in the same site where the furnace is operating but also by other customers of the same utility company connected to the system, even at remote locations.

In the last twenty years the number of electric arc furnaces has increased considerably in the steel producing countries. The increased number of mini-mills has generated a renewed awareness of the impact of electric furnaces on the power system.

Disturbances produced in electrical networks by arc furnaces may be able to significantly affect the quality of energy distributed by electrical companies. An arc furnace is a non-linear, time-varying load, which gives rise to both voltage fluctuations and harmonic distortion. The former phenomenon causes luminosity variations of lamps, the flicker effect, which may give trouble to the human visual system. [1] The detrimental effects of harmonics in power systems are widely known and to mention them will be redundant.

Melting cycles of arc furnace are characterized by strongly time-varying electrical behavior. Quick variations of current and reactive power, which cause flicker, as well as generation of harmonic currents with almost continuous spectrum, whose amplitude changes with time and phase, are associated to normal furnace operation. Time variations of electrical quantities are due to arc-length fluctuations, which can be caused by electromagnetic forces, collapses of metal scraps and electrodes movement activated by regulators. As a consequence, the arc furnace constitutes a considerably unbalanced load, quickly varying between short circuit conditions, when electrodes make contact with scrap metal, and open circuit (arc extinction). [1]

As a general rule of thumb, the ratio of the arc furnace MVA to the utility available short circuit MVA can yield some insight into the likelihood of potential problems. In general, the higher the ratio the better, but a ratio of 80 or larger is sometimes used as a guideline to determine if serious study efforts are required. Where voltage flicker is a problem, or the likelihood of a problem caused by an electric arc furnace addition is high, the solutions are normally difficult and/or expensive. [4]

IV.2 Modeling of Electric Arc Furnaces

A very accurate model of EAFs has been developed by researchers at the University of Bologna & Polytechnic Institute of Milan (Italy). The model has been used extensively in computer simulations and was implemented with EMTP, including the UIE flickermeter. Since the arc furnace constitutes a highly unbalanced load it was better represented in a three phase model contrarily to previous models who worked only with single phase models.

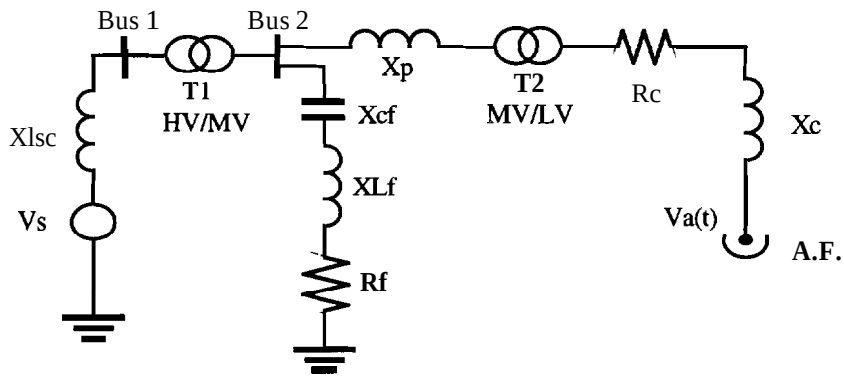

Fig. IV.1 Single phase equivalent diagram.

Bus 1 is the point of common coupling **(PCC). T1** is the high voltage-medium voltage transformer, **T2** is the medium voltage-low voltage transformer, with secondary adjustable voltage. Xlsc is the short-circuit reactance at the PCC, Xp the series reactance inserted for flicker compensation, Xcf, **Xlf** and **Rf** are the equivalent capacitance, reactance and resistance of the harmonic filters for distortion compensation, Xc and Rc are reactance and resistance of the connection line between furnace electrodes and T2. The HV/MV and MV/LV transformers (220121 kV Y-Y, 21/0.9∏0.6 kV Y-D) have rated power 95 and 60 MVA respectively. The maximum power absorbed by the furnace is 60 MVA. [1]

The voltage at the electrodes terminals **Va(t)** is modeled by a set of harmonic voltage sources (odd harmonics up to n = 15) whose amplitude is modulated by a factor **k(t)** that takes into account the arc length variations. $Va(t) = k(t)\sum_n a_n \cos(n\omega t + \varphi_n)$

The selection of the modulation factor **k(t)** gives place to two different **models.** In the first case the arc-length variations are assumed to be sinusoidal, and hence **k(t)** is a sinusoid of frequency between 0.5 - 25 Hz. Include is the range where **maximum** sensitivity of human eye to luminous fluctuations occurs. The second case is a probabilistic model that represents the arc-length variations as band limited white noise.

The main results of the simulation (base case) are AVN at the point of common coupling (PCC), total harmonic distortion and spectrum of voltages & currents at the different buses.

Comparing the results with actual field measurements in steel plants in Northern Italy, the deterministic model (sinusoidal variation law) provides worst case **approximations** which enable determination of maximum flicker sensation [1]. The results of the white noise variation law model, according to the authors, seemed more realistic **and** closer to the average field measurements.

IV.3 Flicker Measurement

The following is a sample waveform of a sinusoidal quantity modulated by another sinusoid of smaller frequency and amplitude.

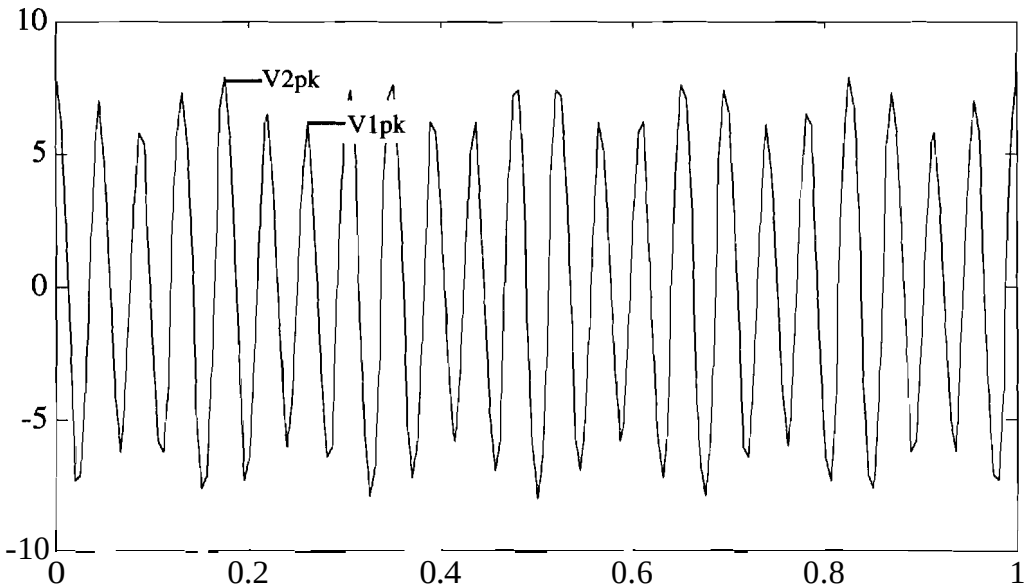

Fig. IV.2 Amplitude Modulated Wave

For voltage waveforms, voltage flicker is usually expressed as the RMS value of the modulating wave divided by the average RMS value of the entire waveform. It is also expressed as the change in voltage divide by the voltage (AVN). [4] Another :namefor ΔV/V is severity of voltage flicker (Pst).

Mathematical relations for Fig. 2:

$$\Delta V = V_{2pk} - V_{1pk}$$

$$\text{RMS Voltage of Modulating Wave} = \frac{\Delta V}{2\sqrt{2}} = \frac{V_{2pk} - V_{1pk}}{2\sqrt{2}} \quad \text{(A)}$$

$$\text{Average RMS Voltage} = \frac{V_{2pk}/\sqrt{2}}{2} + \frac{V_{1pk}/\sqrt{2}}{2} = \frac{V_{2pk} + V_{1pk}}{2\sqrt{2}} \quad \text{(B)}$$

$$\text{Percent Voltage Flicker} = \frac{\text{(A)}}{\text{(B)}} \times 100 = \frac{V_{2pk} - V_{1pk}}{V_{2pk} + V_{1pk}} \times 100$$

IV.4 SCVD Calculations

Using this technique, the severity of voltage flicker can be estimated based on the maximum furnace rating (MW) and the available short circuit MVA at the point of common coupling (PCC). A quantity to measure voltage flicker is defined as Short Circuit Voltage Depression (SCVD): [4]

$$\text{SCVD} = \frac{2 \times \text{MW rating of furnace}}{\text{MVA sc at pcc}}$$

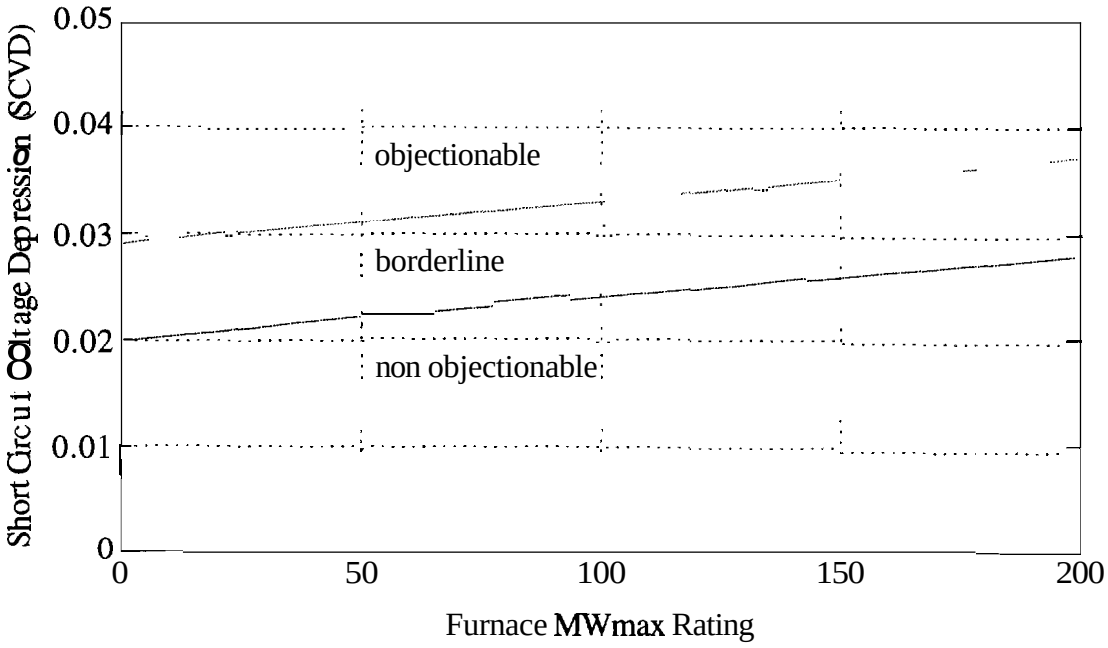

Fig. IV.3 SCVD as a function of furnace MWmax

The curves shown in Fig. 3 were derived from data compiled by UIE (International Union for Electroheat) and UNIPEDE (International Union of Producers and Distributors of Electrical Energy). This plot shows the acceptability of flicker produced by a furnace based on its maximum MW rating and SCVD. [4]

IV.5 Flicker Tolerance & Limits

There are no established standards defining acceptable voltage flicker levels that are used consistently and uniformly in the power industry today in the United States. Each utility has its own standard or guideline based on their individual experiences with the voltage flicker phenomena.

The establishment of a tolerance threshold is subjective, since it is influenced by many variables. Factors affecting the determination of a limit for flicker can include ambient lighting levels, size and type of lamp, room decor, length in time and the abruptness of the voltage variation, and the intensity and immediate occupation of interest of the observer.

The IEEE Std. 519-1992 "IEEE Recommended Practices and Requirements for Harmonic Control in Electrical Power Systems" addresses and includes curves of perceptible and objectionable flicker derived from empirical studies (dating back to 1925, 1934, 1958 & 1961). Revised and updated curves should be available by 1995.

The IEEE Std. 141-1993 "IEEE Recommended Practice for Electric Power Distribution for Industrial Plants" (The Red Book) also discusses the issue with ranges of observable and objectionable voltage flicker. [4]

The problem is further compounded by the fact that fluorescent and other lighting systems have different response characteristics to voltage changes. For example, incandescent illumination changes more than fluorescent, but fluorescent illumination changes faster than incandescent. [9]

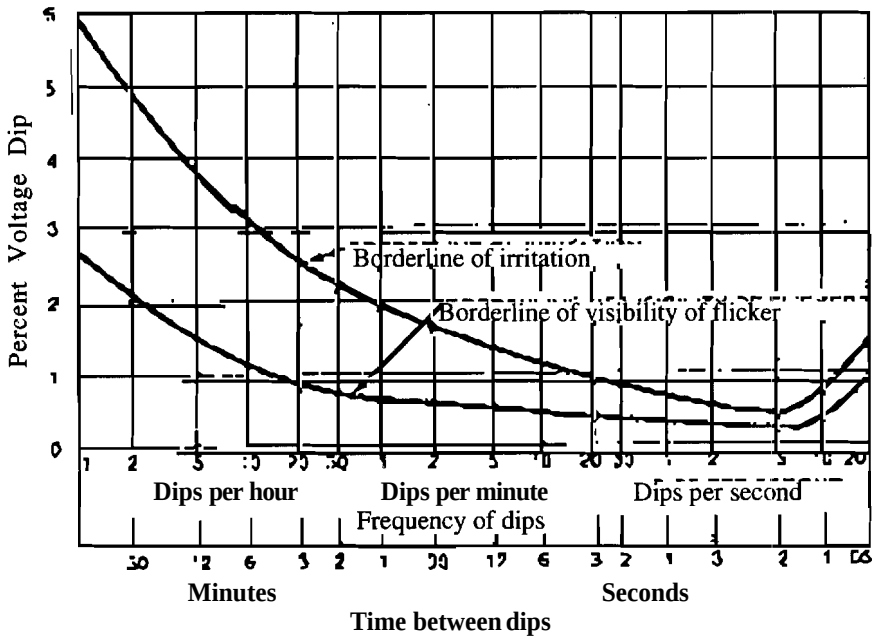

Fig. **IV.4** Range of observable and objectionable voltage flicker versus time

Fig. **4 (*)** shows acceptable voltage flicker limits for incandescent lights used by a large number of utilities. It can be noticed that the maximum sensitivity occurs between **5-10** Hertz. **(*)** From IEEE Std. **141-1993** (The Red Book). [9]

Neither of the aforementioned industry standards treats the effects of voltage flicker on fluorescent lamps. This issue was analyzed by a study that Southern California Edison Company performed in a steel plant from one of their customers. **A** thorough description of the study and its results and an interesting discussion on the subject are available in reference 7.

Methods for Reducing Electric Arc Furnace Disturbances

IV.6 Stiff Source

Probably the most drastic way to reduce voltage flicker is to make the source so stiff that the load variations will not be reflected at the point of common coupling.

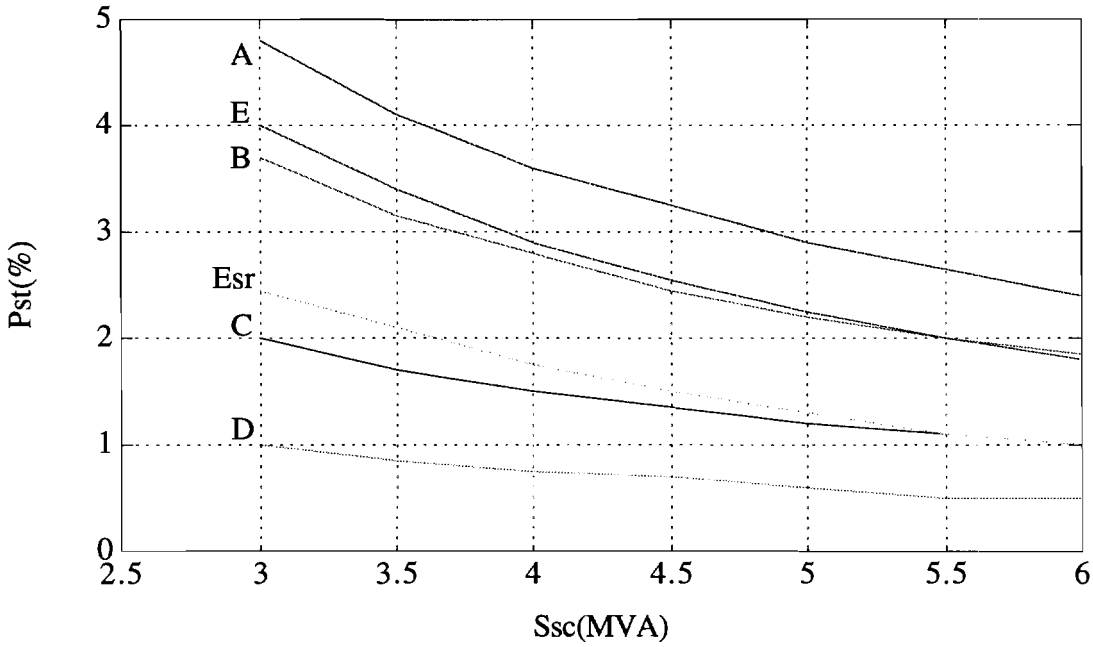

Fig **IV.5.**

Fig. 5: Experimental and simulated curves showing the behavior of maximum Pst as a function of the short-circuit power at the point of common coupling, with and without series reactance (for flicker compensation). Simulations refer to both sinusoidal (curves A & B) and white-noise (curves C & D) arc-length variation laws. Curves E & Esr are taken fiom experimental data. A, C & E are obtained in the absence of series reactance [1].

Ssc: apparent power at bus 2 when furnace is in short circuit conditions.
Pst: short term flicker severity (AVN).

However, to increase the system short-circuit capacity usually is very difficult and expensive. Besides, the Ssc of a an electrical distribution system is not constant, it varies throughout the day depending on the numbers of generating units on line and transmission lines in use. Nevertheless some viable options can be grouped in this category, for example to feed the arc furnace directly fiom a high voltage line, without an intermediate transformer.

Also using a DC arc furnace will reduce the flicker severity for the same given capacity. It is generally accepted that the voltage fluctuations for DC arc furnaces are approximately one half to one third of that of equivalent AC arc furnaces. However, a DC furnace will be more expensive since it requires an additional high power rectifier circuit.

IV.7 Static Var Compensators

Static Var Compensators (SVCs) are capable of supplying the quick changes of reactive power needed by rapidly changing loads like arc furnaces. SVCs provide an effective voltage regulation with very quick response times. Nonetheless they are among the most expensive systems for flicker control and generate the so called pole frequencies that can interact with the system adding another power quality problem, specially if the added signals are near the resonant frequency of the network. The latter can be overcome by means of a filter tuned at the offending frequency. In some cases, depending; on the configuration, the SVC may generate less amount of pole frequencies or frequencies of a higher range that need less filtering.

IV.8 Series Active Filters (SAFs)

The authors of this investigation try to use the SAF as a series capacitor to suppress flicker in an arc furnace supply system, in which the value of capacitance is continuously adjusted to correspond to the variations of reactive power in the load. The SAF can behave not only as a series active capacitance but also as a voltage harmonics filter. [5]

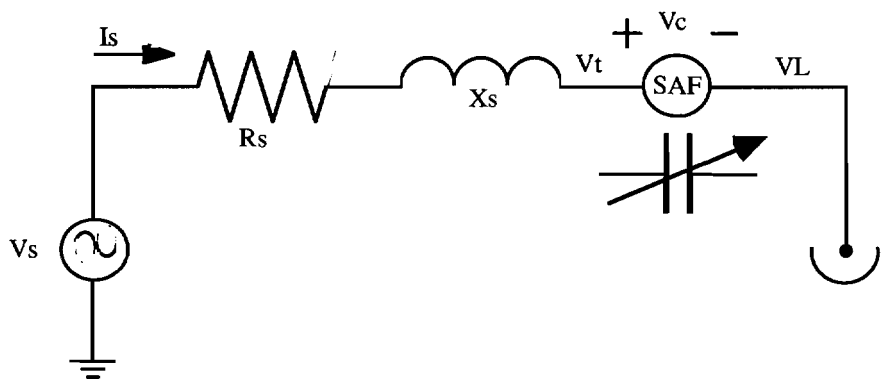

Fig. IV.6 Single phase equivalent circuit of proposed system.

The SAF and system were simulated in a single phase model with the load of an 80 ton steel melting arc furnace. The results are measured with a flicker compensation coefficient h , defined as:

$$\eta = \frac{\Delta V_{10T} - \Delta V_{10L}}{\Delta V_{10T}} \qquad \frac{\Delta V_{10T} : \Delta V_{10} \text{ of } V_T}{\Delta V_{10L} : \Delta V_{10} \text{ of } V_L}$$

$\Delta V10$ is evaluated during 400 msec.

	PAF	SAF
h	83.4 %	92.0 %

The authors developed a downsized single phase prototype system with a 200 Vrms voltage source in which the load is simulated by a microprocessor controlled current source. The microprocessor keeps an arc furnace load current data pattern of 360 msec and outputs the current reference to a linear current amplifier. The compensator is also simulated by a microprocessor controlled voltage amplifier.

The SAF can be applied not only as a flicker compensator in arc furnace supply systems, but also as a power system voltage stabilizer for flexible AC transmission systems (FACTS).

IV.9 Another proposed Static Var Compensator

Basic operating principle.

In Fig. 7, Q1 and Q2 represent two self commutated bidirectional switches with complimentary gatings. Switch Q2 is used to free-wheel the inductor current. Through high-frequency switching, the fundamental component of the inductor current IL can be controlled. Fig. 8 shows the voltage and current waveforms of the circuit. [ti]

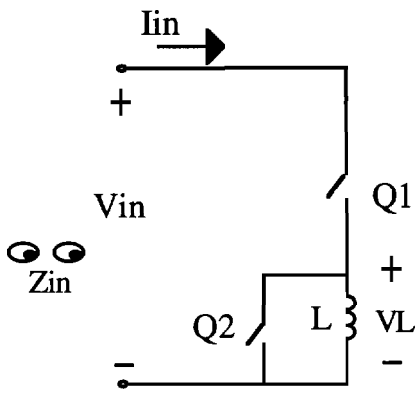

Fig. IV.7

If the effect of high-order switching harmonics is neglected, the inductor voltage and input current can be expressed as:

VL = VinxD Iin = ILxD

where D is the duty cycle of switch Q1. Given the inductor reactance as ZL = VL/IL = wL and w being the fundamental frequency in radians/second, the equivalent reactance seen from the input becomes:

Zin = Vin/Iin = (VL/D)/(ILxD) = ZL/D^2

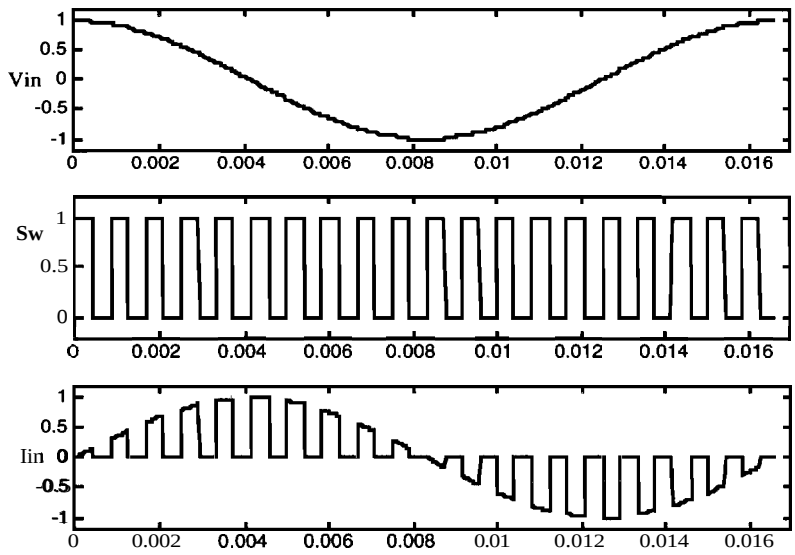

Fig. IV.8

The last equation shows that the input equivalent reactance can be expressed as a function of the inductor reactance and the switching duty cycle. In other words, the reactive power of this circuit can be adjusted through duty cycle control. [6]

Actual Compensator Circuit

A three-phase six-pulse PWM ac converter has been identified for this particular application.

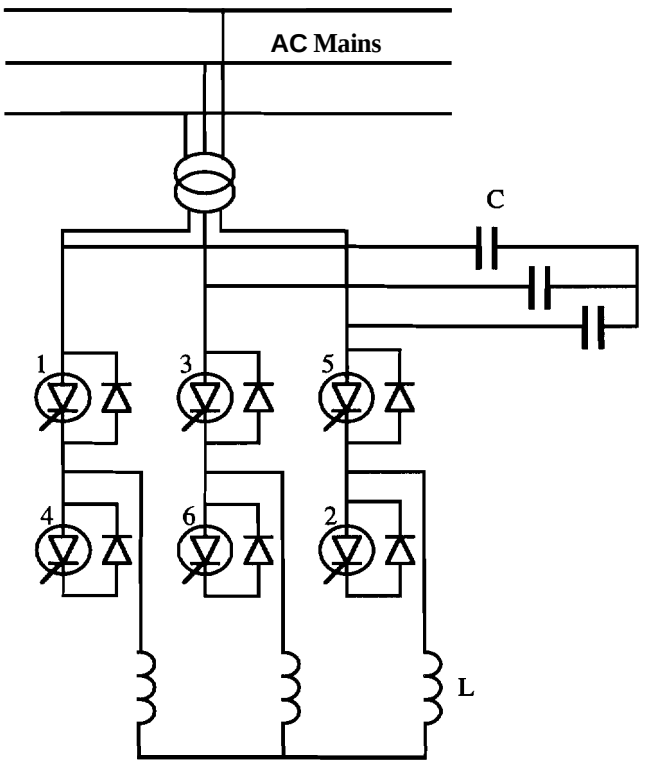

Fig. IV.9

In Fig. 9 a transformer is used for isolation and voltage matching purposes; and shunt capacitors are used to provide leading reactive power. The upper three switches are controlled with the same gating signal while the lower three switches are gated complementarily. Due to high-frequency modulation, harmonics are generated. Since these harmonics are in relatively high orders, less filtering is required as compared to TCR-based compensators. The leakage inductance of the transformer together with the VAR-generating capacitor can be used to form a low-pass filter. This eliminates the use of additional filters and further simplifies the overall compensator structure. [6]

IV.10 Harmonic Filter Tuning and its effects on Voltage Flicker

In order to apply power factor correction to a furnace circuit, capacitor banks are normally applied in a tuned filter configuration. Single-tuned passive filters are common, where a reactor is added in series with the capacitor bank producing a tuned circuit at one frequency. This allows the application of the capacitor bank on the same circuit as a harmonic rich source. It also provides a low impedance path for a selection of the harmonics, therefore resulting in a reduction of the overall circuit harmonic distortion. [4]

The application of a filter bank results in a low impedance at the tuned frequency and a higher impedance at a lower, parallel resonant frequency. The installation must be carefully engineered to place the parallel resonance at a point that does not result in harmonic overvoltages during energization of the furnace transformer or the steady state operation of the furnace. [4] In other words, care should be exercised when using tuned filters from the fact that a significant harmonic frequency generated by the arc furnace (or the transformer) could be close to or the same as the filter's resonant frequency. This would lead to enhanced harmonic distortion. This can be avoided by proper selection of the filter.

IV.11 Flicker Compensation with Series Reactance

The simulation model in Fig. 1 was used to investigate the effectiveness of a, solution for flicker and harmonic distortion compensation consisting of series inductors and shunt filters, inserted at the MV side of the furnace transformer (T2).

Simulations were made with different series inductor and filter ratings, adjusting the secondary voltage of the MV-LV transformer in order to keep constant the mean active power absorbed by the furnace. Different values of short-circuit ratio, SCR (defined as the ratio of the short circuit power at PCC to the maximum plant apparent power), where also considered, in order to point out its influence on the effectiveness of the compensation system investigated. [1]

The flicker compensation effect provided by the series inductor can be explained considering that an increase in furnace-side voltage, due to insertion of series inductor, causes arc lengthening. According to on-field observations, the maximum arc-length variations, ΔL, was considered independent of arc length in the range of values used for

the simulations. Hence longer arcs provide smaller variation of relative length ΔL/L and, consequently, of arc voltage. [1]

Again, the UIE flickermeter was implemented in EMTP for the purpose of model validation. Calculation of the quantity recommended by IEEE 519 to evaluate the amount of harmonic distortion which affects the voltage and current, that is, the Total Harmonic Distortion (THD), is not straightforward, due to the presence of characteristic and non-characteristic harmonics, as well as interharmonics. According to the actual meaning of THD, which measures waveform deviation from sinusoidal shape, the effect of interharmonics generation, which is computed by flicker measurements, was not taken into account in the expression for THD estimation, that is,

$$THD = \frac{\sqrt{\sum_{h=2}^{N} A_h^2}}{A_1} \times 100\%$$

where Ah is the amplitude of multiple harmonic voltages or currents, A1 is the amplitude at the fundamental frequency (50 or 60 Hz), N is normally lower than 50.

where Ah is the amplitude of multiple harmonic voltages or currents, A1 is the amplitude at the fundamental frequency (50 or 60 Hz), N is normally lower than 50. [1]

Table IV.1 summarizes the results of several simulations aiming at detection of compensation possibilities offered by the investigated solution for the electrical plant in question (see section 2). As can be seen, both flicker (measured at Bus 1) and voltage THD (measured at Bus 2) can be considerably reduced. Comparing the value of Pst in the presence and absence of filter, it comes out that the filter itself does not give any contribution to Pst compensation (actually, it slightly increases Pst). This is due to the different frequency ranges responsible of the two phenomena, that is, low frequencies for flicker, which are able to affect filter-capacitor voltage, and higher frequencies for harmonic distortion. [1]

Moreover, it is interesting to observe that insertion of series reactance without filters does not give any reduction of harmonic distortion, as occurs when the load is constituted by AC/DC converters. On the contrary, an increase of current and voltage distortion at bus 2 is detected. This can be explained by the arc-length enhancement which follows the feeding voltage adjustment needed to keep constant the furnace active power when series inductor is inserted. [1]

Xp ohms	THD(Vb)	THD(Va)	THD(I)	Pstb %	Psta %
0	1.16	0.5	3.01	1.73	1.79
2.02	1.29	0.58	3.29	1.53	1.57
3.58	1.42	0.59	3.41	1.38	1.42
4.78	1.57	0.6	3.6	1.26	1.4
5.71	1.68	0.67	3.75	1.08	1.13
6.51	1.78	0.83	3.89	0.85	0.88

Table IV.1

(*) 'b' denotes measurement before filter insertion, 'a' denotes after.

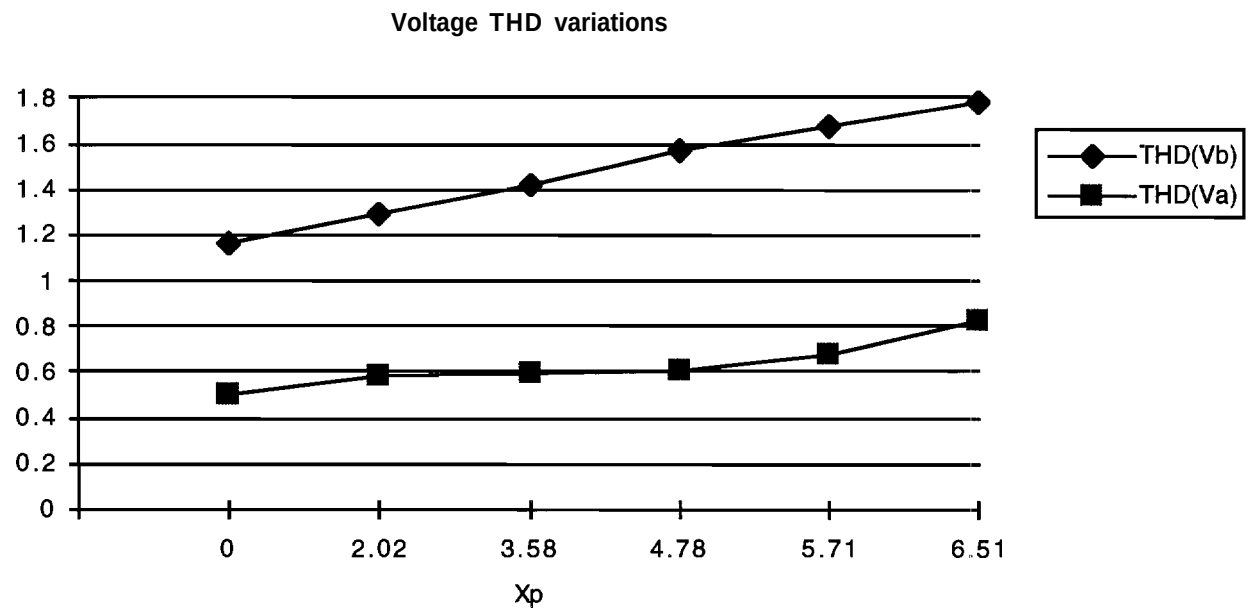

Fig. IV.10

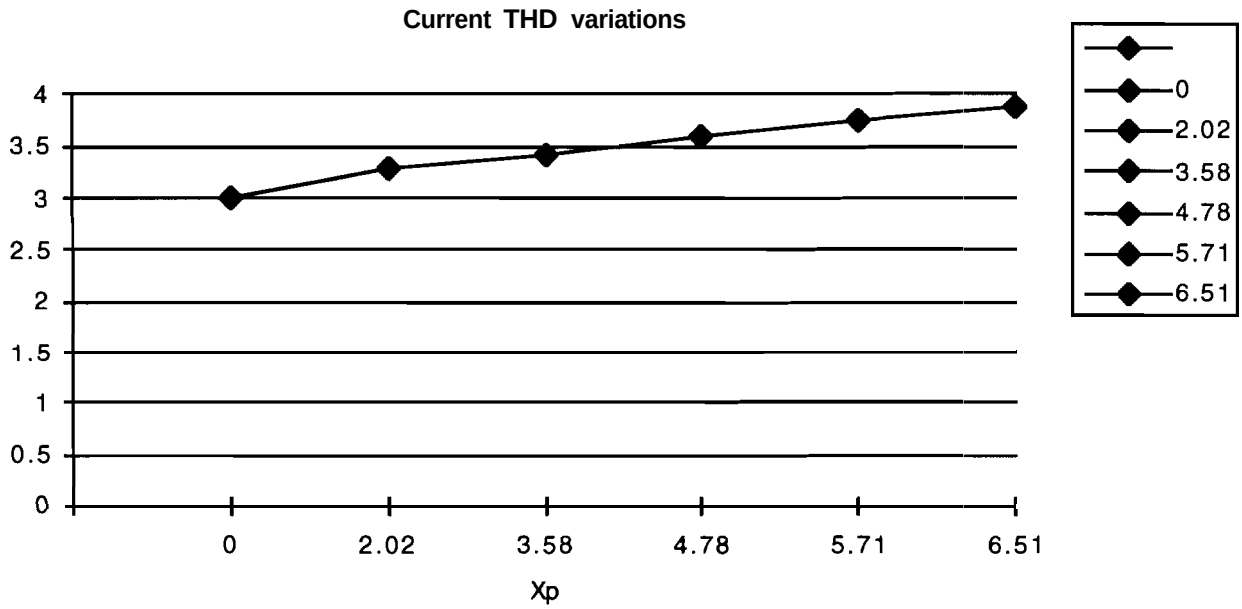

Fig. IV.11

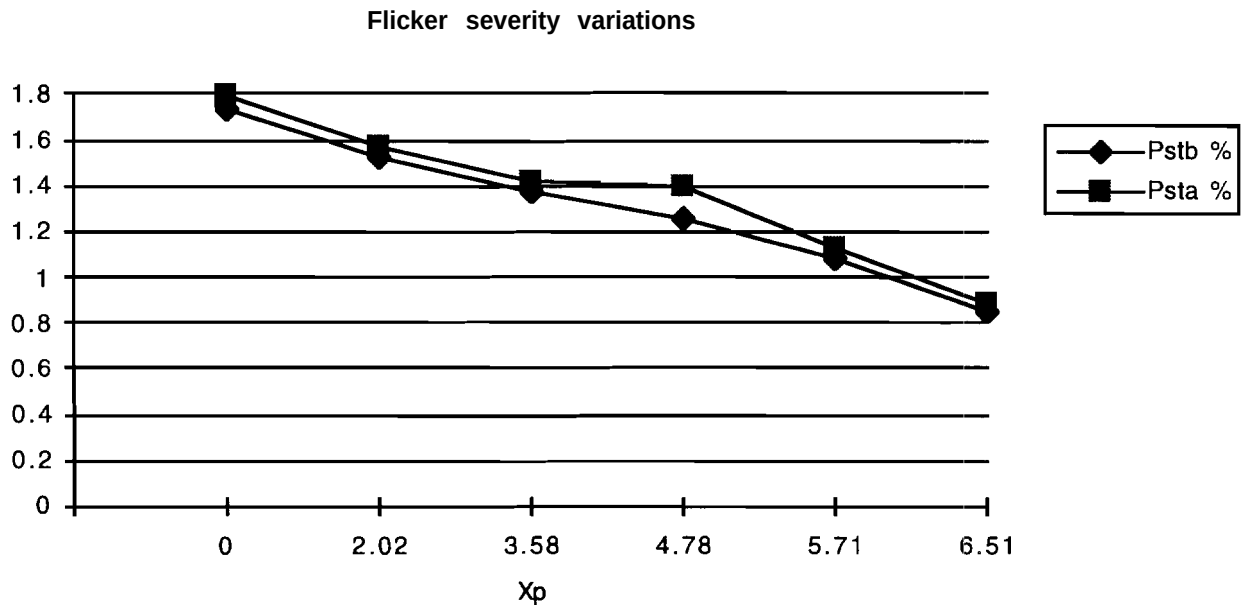

Fig. IV.12

IV.12 Conclusions

The task of flicker compensation in an electric arc furnace supply plant is a fairly difficult one even for a small capacity system. The problem of the flicker disturbance is not only that of a non-linear load, since the arc furnace has nonlinear and time-varying V-I characteristics. Besides containing a strong presence of specific harmonic frequencies, like the dreaded third and fifth harmonics, the furnace generates almost a continuous spectrum from DC up to the kilohertz range. In some cases simple harmonic compensation techniques are not enough to reduce the variations in the electrical quantities.

The insertion of a series reactance along with the use of passive filtering seems to offer a relatively inexpensive (compared to others) method of flicker compensation. Nonetheless the simulated results and actual measurements show a trade-off between flicker severity and THD that could be problematic in bigger systems.

The use of passive (harmonic) filters can provide compensation for the harmonic distortion that arc furnaces and transformer's inrush current cause. However, the flicker disturbance can not be taken care of with passive filters only, moreover, extra care is needed due to the parallel resonant condition of the filter.

Static Var Systems (SVSs) are about the most sophisticated method of dealing with disturbances originated from rapidly changing loads. They provide a quick response that can follow up with the rapid variations of the electrical quantities. The disadvantages of SVSs are their high cost and the presence of pole frequencies inherent to some configurations.

Besides actual measurements of voltage and current, the analysis of a furnace supply system requires other tools such as (specific) harmonic and flicker measurements and frequency spectrum analysis among others. These tools will allow the power engineer to have a better perspective of the power quality problem at hand.

Also simulation programs have proven to be a very effective tool in the analysis of these systems as they have become more accurate than ever before. Any major study of an existing arc furnace supply system or design of a new one would be incomplete without it.

IV.13 References

[1] G.C. Montanari et al, "Flicker and Distortion Compensation in Electrical Plants Supplying Arc-Furnaces", Proceedings of the 1994 IEEE Industry Applications Meeting, Vol. 3.

[2] G.C. Montanari et al, "Arc-Furnace Model for the Study of Flicker Compensation in Electrical Networks", IEEE Transactions on Power Delivery, Vol. 9, No. 4, October 1994.

[3] G.C. Montanari et al, "The Effects of Series Inductors for Flicker Reduction in Electric Power Systems Supplying Arc Furnaces", Proceedings of the 1993 IEEE Industry Applications Meeting, Vol. 2.

[4] S.R. Mendis, M.T. Bishop, J.F. Witte, "Investigations of Voltage Flicker in Electric Arc Furnace Power Systems", Proceedings of the 1994 IEEE Industry Applications Meeting, Vol. 3.

[5] A. Nabae, M. Yamaguchi, "Suppression of Flicker in an Arc-Furnace Supply System by an Active Capacitance", IEEE Transactions on Industry Applications, Vol. 31, No. 1, Jan/Feb 1995.

[6] H. Jin et al , "An efficient Switched-Reactor/Capacitor-Based Static VAR Compensator", Proceedings of the 1992 IEEE Industry Applications Meeting.

[7] B. Bhargava, "Arc Furnace Flicker Measurments and Control", IEEE Transactions on Power Delivery, Vol. 8, No. 1, Jan. 1993.

[8] D. Andrews, M.T. Bishop, J.F. Witte, "Harmonic Measurements, Analysis, and Power Factor Correction in a Modern Steel Manufacturing Facility", Proceedings of the 1994 IEEE Industry Applications Meeting, Vol. 3.

[9] IEEE Std. 141-1993, "Recommended Practice for Electric Power Distribution for Industrial Plants" (The Red Book).

Chapter V

Transformer Inrush Currents in Power Systems

David Stenberg

V.1 Introduction

The phenomenon of transformer inrush current was discovered and analyzed as early as 1892. Since this time, there have been many studies looking at the cause and effects of this phenomenon. The earlier studies concentrated on finding the magnitude of the waveform and did not look at other characteristics such as the shape of the waveform.[1] Their main motivation for determining this value was to avoid system failure due to the tripping of relays or blown fuses. More recent studies have looked at the shape and other characteristics of the waveform because the DC component of the inrush waveform has been found to cause disturbances in telecommunication systems.[1] The reason for the concern with this transient current is that it can reach values in the range of 10 times the rated value of current during the energization of the transformer.

V.2 The Cause of Transformer Inrush Current

Transformer inrush current is ultimately caused by its nonlinear characteristics. In order to better understand this, a closer look at the fundamental characteristics of a transformer is required. The job of a transformer is to step up and down the values of voltage and current, and to provide electrical isolation between sides of the transformer. This task in the steady state is accomplished very effectively and the ratio of the voltages and currents

are extremely close to the turns ratio of the transformer. However, the transient case is much different. The best way to demonstrate this is to look at the magnetizing characteristics of the transformer. This is shown in Figure V.1.[1]

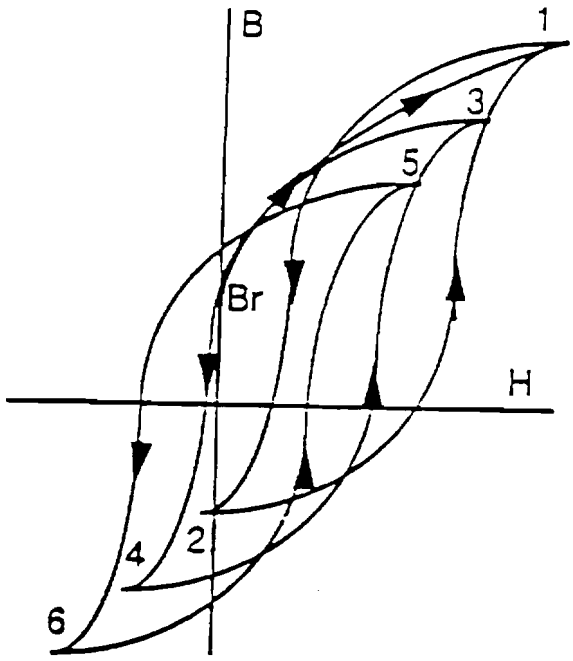

Figure V.1 The Magnetizing Characteristics of a Transformer.

The level of B is proportional to the flux, Φ, and H is proportional to the magnetizing current, i. In order to understand how a transformer reacts during energization, one has to look at the transformer during the de-energization. When a transformer is de-energized, there exists a residual flux density that corresponds to the value of B when the magnetizing current returned to zero upon de-energization. This value is noted in Figure V.l as B,. When the transformer is again re-energized, the transformer will follow the curves shown in Figure V.1. Assuming that the exciting voltage begins magnetizing the transformer core in the same direction as the sign of B,, the core will be magnetized into complete saturation mode corresponding to point 1 on Figure V.1. Once the exciting

voltage returns to a sufficient negative value, the core will become unsaturated and the current will begin to decrease along with the flux to a terminating point designated by point 2. The excitation voltage will again become positive and will drive the core into saturation and the current will begin to increase, this time to a slightly lower value since the flux density was increased from a lower value on the B-H curve. The current will reach a peak corresponding to point 3 in Figure V.1. The transformer will continue to go through this type of excitation until the transients become completely damped out. There will be several peaks of the current, each smaller than the previous one.

Another way to look at this phenomenon is to look at the values of the flux density, voltage and current vs. time. Plots of these waveforms during the de-energization to re-energization are shown in Figure V.2. [2]

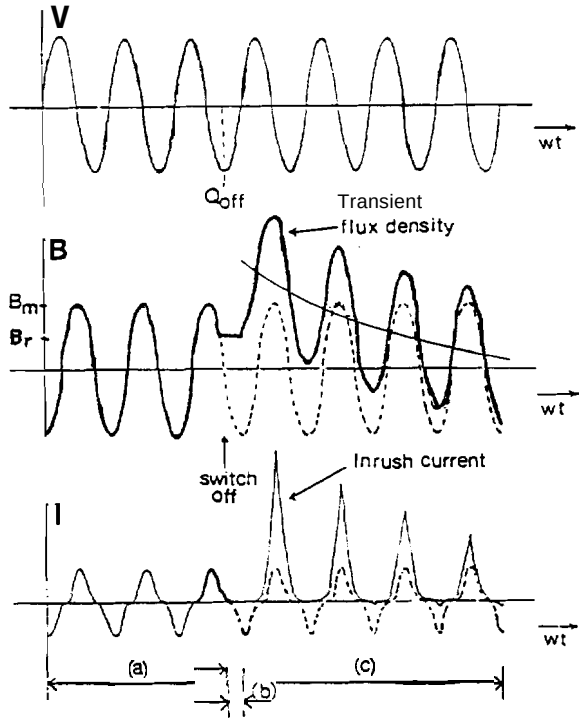

Figure V.2. Energizing Voltage, Flux Density, and Current vs. Time during (a) steady state, (b) de-energization, and (c) re-energization..

Here, the transformer began in steady-state operation. It can be seen that the relationship between the flux density and the energization voltage is one in which the two waveforms are proportional in magnitude and out of phase by 90°. Once the transformer was de-energized, the residual flux that remained in the transformer corresponds to the residual flux density, B_r. When the transformer is again energized, this residual flux is still present. For the case shown in figure V.2, the voltage is near its minimum value at this point and therefore will have to travel the full peak to peak distance which will drive the core completely into saturation. This can be seen from the plot of the flux density after re-energization which corresponds to interval c of the graph. This method of looking at this phenomenon demonstrates the dependence of the magnitude and sign residual flux of the transformer upon de-energization. If the transformer had been re-energized at a point on the flux density and voltage waveforms identical to that of the de-energizing point in both sign and magnitude, the residual flux would be the amount needed to keep the flux density along its normal path and there would theoretically be no inrush current. [2]

V.3 Effects of Transformer Inrush Current on the Power System

This inrush current could potentially affect several things on the power system. One of these is the tripping of the protective relays due to the energization of a transformer and not a fault on the system. This could occur because as the inrush current reaches its peak value, there could be a momentary dip of the voltage that could cause a differential relay to trip out.[2] The inrush current could also cause the malfunctioning of ground fault equipment due to the fact that it can take quite some time to completely decay. [3] One way to potentially fix this problem is to predict the type of the waveform and keep the

relay from tripping during energization of the transformer. However, using the predicted shape and magnitude of this waveform to desensitize relays defeats the purpose of the relays since there could potentially be a fault due to insulation failure during the energization of the transformer. Another potential problem that arises from inrush current is due to the recent push for digital protection of power transformers.[4] The programming of micro-processor based relays requires very accurate modeling of the fault and inrush currents, and the shape and magnitude of this waveform has many factors that it depends on and can be hard to predict. Another potential problem is that the transformer inrush current could cause a fuse to blow if the transient is large enough and lasts for a long enough duration. Potentially, this could cause other circuits to be overloaded and other lines could also be tripped out as well if the system protection system is designed poorly. Another recent effect that has been discovered is that transformer inrush current can potentially cause disturbances in the telecommunication systems. This could effect the communication that links substations for protective relaying systems as well as other communication signals.

V.4 Solutions to the Problem of Transformer Inrush Current

Due to these potential undesired effects of transformer inrush current, there is considerable importance placed on preventing any problems that could arise from it. One solution is to accurately predict the magnitude and shape of this waveform. Simulation of the transformer depends on an accurate model. The single phase transformer is the simplest to understand. Therefore, the simulation of a 1201240 Volt, two winding transformer was done using Simulink, which is a simulation feature of Matlab. The model

that was used was the equivalent-T circuit which is shown in figure **V.3.** The primary side voltage and currents, v_1 and i_1, are shown on the left side. The resistance., r_1, represents the resistance of the primary winding, and the inductance, L_{l1}, is the leakage: inductance of the primary side, which represents the paths of flux that exist that link only the primary winding. The magnetizing inductance, L_{m1}, represents that paths

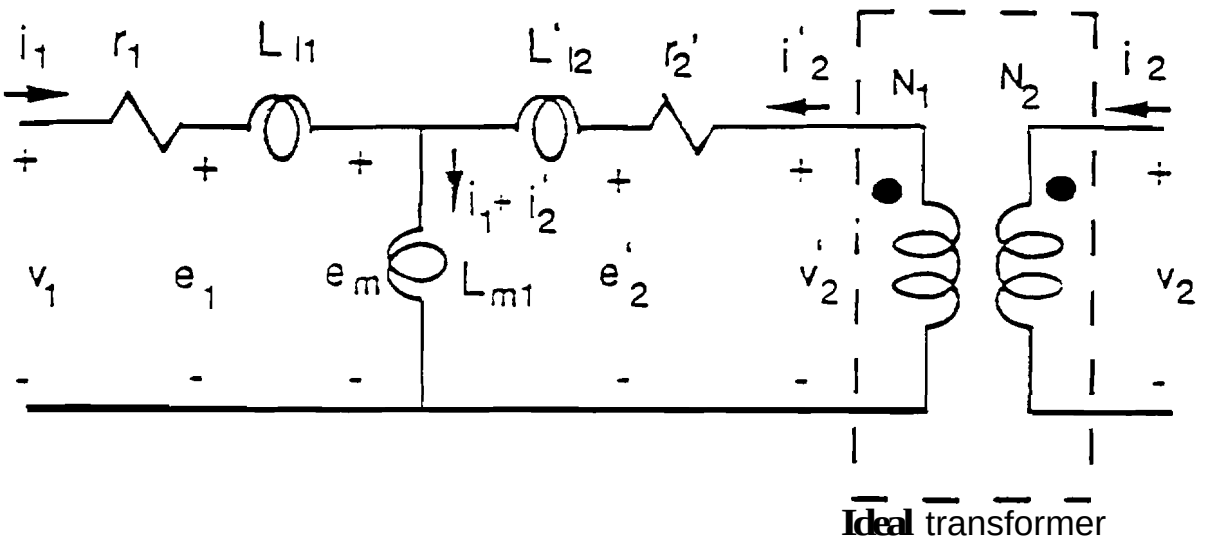

Figure **V.3** The Equivalent-T circuit of the Single Phase, Two Winding Transformer Model.

of flux that link both the primary and secondary windings. The resistance and inductance, r_2 and L_{l2}, are the resistance of the secondary winding and the leakage of the secondary winding which are referred to the primary side of the transformer using the turns ratio of the transformer. The voltage and current of the secondary side are also referred to the secondary side using this turns ratio. The use of the referred quantities is done so that effectively the ideal transformer is not part of the simulation. The first simulation that was

done was with the condition of an open circuit across the terminals of the secondary winding. For an ideal transformer, the current drawn through both the primary and secondary windings should be zero. However, due to the nonlinearity of the transformer, there is an inrush current.

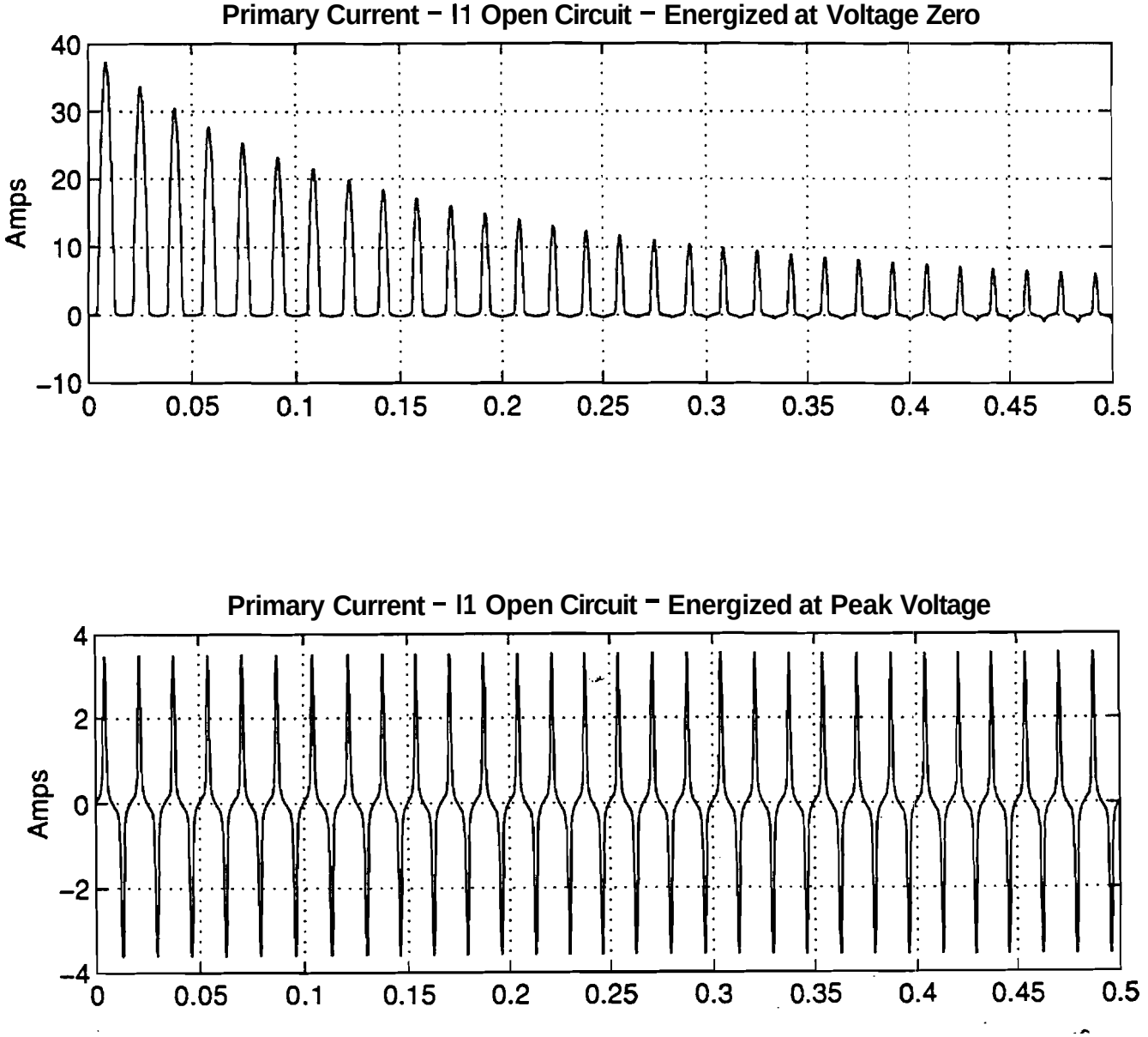

Figure V.4 Simulation Results of the Open Circuit Condition.

The magnitude and shape of this current waveform also varies with the point at which the transformer was energized in relation to the source voltage. Figure V.4 shows the waveforms of the primary current for the open circuit condition for simulation runs of the transformer being energized at the time the voltage source is at zero and at the time the source is at its positive peak. As you can see, these waveforms look very different both in magnitude and shape, even though they were from the same basic conditions of the transformer.The case where the transformer was energized in accordance to the voltage source being at zero gave a current with a peak of nearly 40 amps, and does not decay until nearly 1.5 seconds. For the peak case, there is a very small current, with a peak value of less than 4 amps and a very small rms value since the peaks are very narrow. This waveform does not decay and is more a result of the magnetizing action of the transformer. The other case that was simulated is where a 1.5kVA load at 0.8 power factor lagging was placed across the secondary terminals. The simulation of this case shows that there is an inrush current present when there is a load on the secondary terminals. The shape and magnitude of this waveform is different from the previous simulations that were performed. The primary current reaches a peak value of nearly 60 Amps. From looking at these simulations as well as the background, one can observe that there are several factors that affect the magnitude of the transformer inrush current. The results of this simulation are shown in Figure V.5

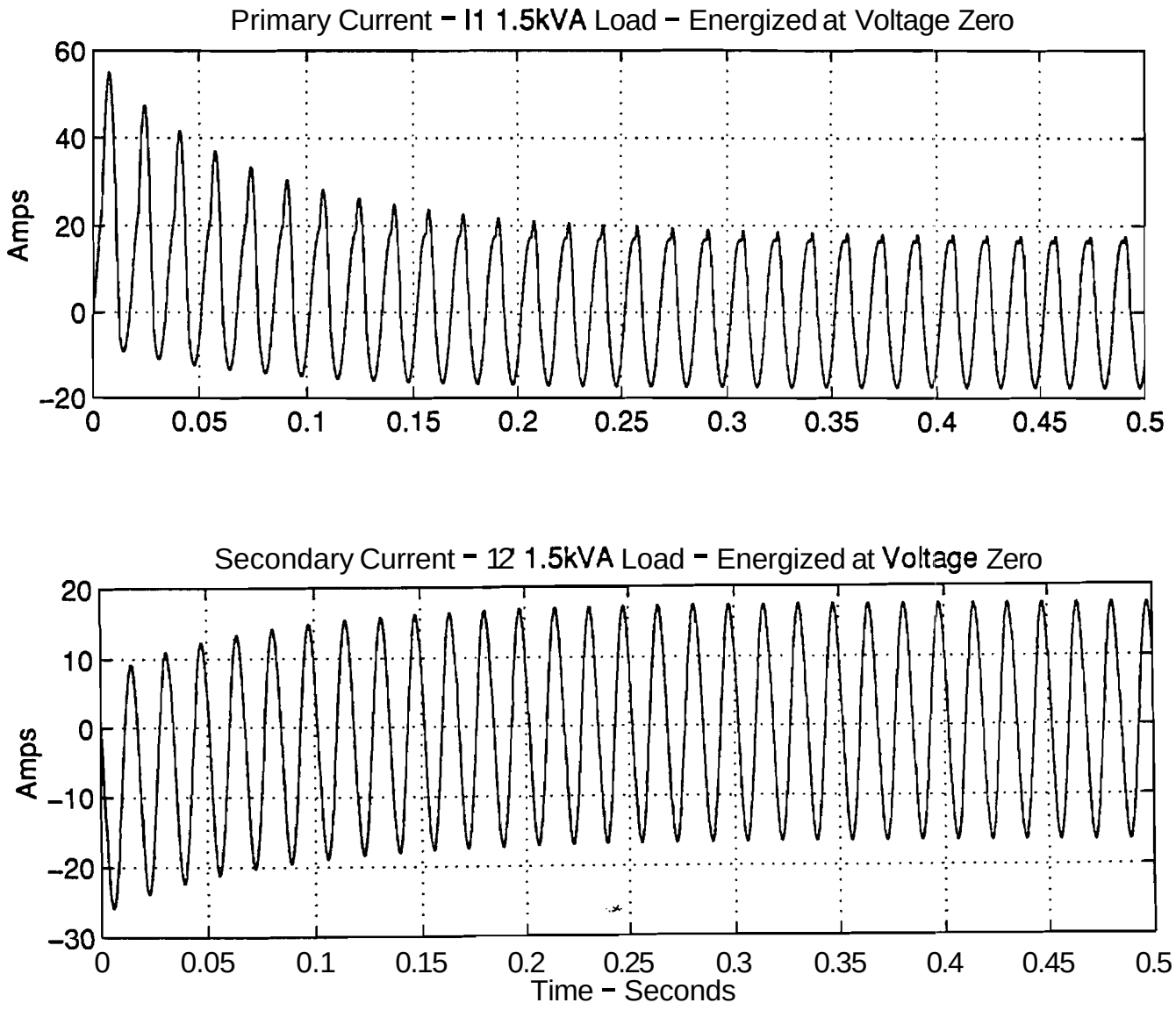

Figure V.5 Simulation Results for the Case of a 1.5kVA Load on the Secondary Terminals.

Another technique used with inrush current, other than the use of simulation in order to predict the transformer inrush current, is to place a capacitor on the secondary terminals of the transformer. This capacitance creates a back emf which cancels out the affect of the

magnetizing flux that is produced during the saturation of the transformer. This further demonstrates the role that the load plays on the magnitude and shape of the transformer inrush current. This technique is often more desirable over predicting the current through simulation, because it actually removes the inrush current. However, there are some applications where this method is not feasible due to the application and simulation must be done in order to be able to predict the currents that will be present during excitation.

V.5 Three Phase Transformers

In the power system, three phase circuits are common. Much of the discussion to this point has looked at the single phase case for the reason of simplicity and there are some differences and considerations that must be looked at when evaluating a three phase transformer. Simulation of a three phase transformer is going to be much more complex due to the close coupling of phases, and therefore, a much more complex model is needed. Also, the phase difference of 120° causes the three phases to be energized at different points in the relation to the peak, which eliminates the possibility of trying to energize the transformer at times where the inrush current will be minimized. [5]

V.6 Factors that Affect Transformer Inrush Current.

As it has been pointed out, there are many factors that affect the transformer inrush current. Table V.1 shows some of these things that affect transformer inrush current.

Factors that affect the Magnitude and Shape of the Transformer Inrush Current Waveform.	
Factor	Action Taken in Order to Reduce the Inrush Phenomena due to this Factor
The Point in Time when the Transformer is Energized Relative to the Voltage Source.	Energize the transformer at the same point that it was de-energized.
The Magnitude of the Voltage Source.	None, since this is not a variable quantity.
Magnetization Curve of the Transformer.	Some consideration is taken during the design stage of the transformer.
The Magnitude of the Residual Flux in the Transformer.	De-Energize the transformer at a point when the flux is zero.
The Sign of the Residual Flux in the Transformer.	Keep track of the sign of this when de-energizing the transformer.
The Presence of a Tertiary Winding	None, since this is a characteristic of the transformer, and the application that it is used in
The Load on the Secondary Side of the Transformer.	Use load balancing capacitors that produce a back emf proportional to the magnetizing flux during the saturation of the transformer at the point of energization.
The Source Impedance and Winding Resistance of the Transformer.	These quantities are varied. somewhat in the design of the transformer.
Transformer Construction Type (i.e. Single Phase, Three Phase Bank, Three Phase - Three Limb Core type, etc.)	For a given application, a single phase or three phase type would be required, but the use of a core, or three single phase transformers in a bank is a choice that can be made to minimize the inrush current.

Table V.1 A Table Showing the Factors that Affect Transformer Inrush current and the Theoretical Techniques that could be used to Reduce the Effects.

V.7 Conclusions

The phenomena of transformer inrush current has been known about for over a century now, and has been looked at for many different reasons. The presence of this inrush current can be explained through the analysis of the nonlinear characteristics of a transformer during both its de-energization and re-energization. There are many factors that affect the magnitude of this inrush current as well as its shape. There are several techniques that are applied in dealing with this phenomenon. One such technique is the accurate simulation of the transformer in order to predict the magnitude arid shape of this current waveform. This technique is affective in learning about the inrush current for various different applications but does not remove the current from the system, and further precautions must be made to protect the system from the inrush (current during energization of the transformer. One method which removes the majority of the current is to place capacitance across the secondary terminals in order to block the inrush current. Because this is the only step in this solution to the problem, it is a popular one where its application is feasible.

BIBLIOGRAPHY

[1] Alyasin, Souheil Z., *"Modeling and Analysis of Distribution Network Transient Waveforms Attributed to the Saturation of Distribution Transformers."* , Master's Thesis, Purdue University, West Lafayette, IN, 1994.

[2] Ling, Paul C. Y. and Amitava Basak, "Investigation of Magnetizing Inrush Current in a Single-Phase Transformer." ***ZEEE Transaction on Magnetics,*** v. 24, n. 6, pp. 3217-3222, Nov. 1988.

[3] Chakravarthy, S. K. and C.V. Nayar, "An Analytical Tool for Studying Transformer Inrush Current." ***International Journal of Electrical Engineering Education,*** v. 30, n. 4, pp. 366-373, Oct. 1993.

[4] Rahman, M. A. and A. Gangopadhyay, "Digital Simulation of Magnetizing Inrush Currents in Three-Phase Transformers." ***ZEEE Transactions on Power Delivery,*** v. PWRD-1, n. 4, pp. 235-242, Oct. 1986.

[5] Yacamini, R. and H. Bronzeado, "Transformer Inrush Calculations Using a Coupled Electromagnetic Model." ***ZEE Proceedings: Science, Measurement and Technology,*** v. 141, n. 6, pp. 491-498, Nov. 1994.

Chapter VI

Nonsimultaneous Pole Closure in Transmission Lines

E. A. Walters

VI.1 Introduction

This chapter discusses the causes and parameters affecting transmission line energization overvoltages. Problems arising from these overvoltages are also presented. Due to the problems associated with these overvoltages, the need for accurate transient transmission line models is introduced. The derivation of a transmission line model is discussed and a study using this model with three different types of pole closure schemes is explored.

VI.2 Causes of Overvoltages

Before a thorough presentation of line energization overvoltages can be made, a brief explanation of overvoltages and their causes must be discussed. In a transmission line which is initially de-energized, if one end of the transmission line is connected to a source (energized) the voltage starts to propagate down the line. Since the line is de-energized, this voltage causes current (charge) to flow down the line. Once this current and voltage reaches the other end of the line, the load constraint controls the current and voltage. In the examples explored in this chapter the load constraint is an open circuit. Therefore, the current at this end must be zero. However, since charge has already flowed to the end of the line, the voltage is doubled at the end of the line to force the charge to flow back down the line. This voltage which can be twice the rated voltage is called a phase-to-ground overvoltage. This is not the only type of overvoltage that can be produced. In a three-phase system, these reflected waves in all three phases can result in large phase-

to-phase overvoltages. These reflected voltages and currents propagate to the source end where instead of having a load constraint of the current being zero, the constraint is that the voltage is fixed by the source. This boundary condition sets up another reflected wave, this time going back to the load. These reflected waves eventually die out to the steady-state conditions due to the losses in the transmission line.

Several parameters control the magnitudes of these overvoltages. Two of the most significant are the point on the voltage wave at which the pole closes and the time interval between closing of the three phases [1]. Both of these effects are presented in the transmission line study in section VI.5. Other parameters affecting transmission line energization overvoltages include the mutual effects between the three-phase lines, the length and losses of the lines, the presence of trapped charge on the line, and the type of source [2].

VI.3 Problems associated with overvoltages

Overvoltages are associated with three major problems. The first problem is the stress caused by the overvoltages on the insulators [3]. This stress can be broke down into two types: phase-to-phase and phase-to-ground. If the overvoltages can be predicted, and the transmission line designed accordingly, the risk of transmission line failure due to overvoltage stress can be reduced.

The second problem with overvoltages is associated with the financial cost of transmission lines. A 10 percent reduction in the insulation requirements can result in a 10 percent savings in the total cost of the line. Additionally, a phase-to-ground overvoltage in the range of two per unit is not economically acceptable for 1000-kV transmission lines.

The third problem associated with overvoltages is in the design of transmission systems. The overvoltages place strict constraints on the line characteristics and terminal equipment capabilities [4]. If these overvoltages are modelled accurately, this can help limit the errors in specifying equipment early in the design of transmission systems.

VI.4 Modeling of Transmission Lines

In the previous section the need to accurately model transmission line overvoltages was presented. This section is dedicated to developing computer representations of three-phase transmission lines which predict transient overvoltages. This model does not use reflection coefficients and can be combined with other power system components in the dynamic modeling of a power system [5].

Before exploring the three-phase example, a single-phase transmission line will be discussed. The equivalent circuit of a differential section of a transmission line is shown in Figure VI.1. The

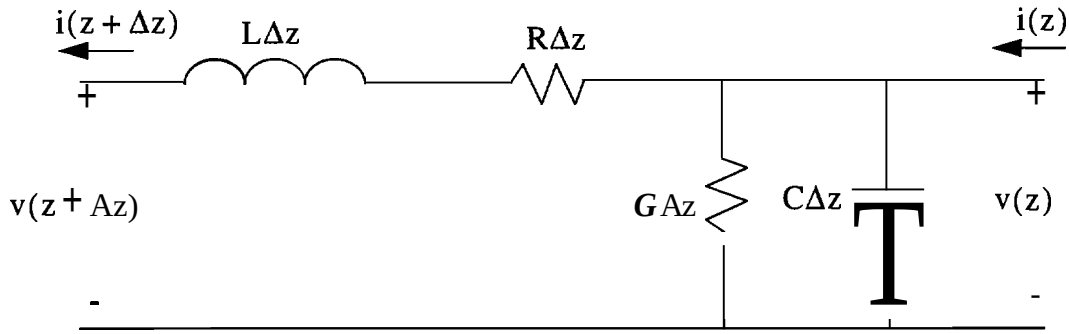

Figure VI.1 Single-phase transmission line differential section equivalent circuit

units of the equivalent circuit parameters are all given in per meter. Using Kirchoff's current law, equation (VI.1) can be obtained.

$$i(z + \Delta z) = i(z) - G\Delta z v(z) - C\Delta z \frac{d}{dt} v(z) \tag{VI.1}$$

By moving $i(z)$ to the left side, dividing on both sides Δz, and taking the limit as Δz approaches zero, (VI.2) can be derived.

$$\frac{\partial}{\partial z} i(z, t) = -Gv(z, t) - C\frac{\partial}{\partial t} v(z, t) \tag{VI.2}$$

By performing Kirchoff's voltage law, a similar relationship can be derived for the voltage which is shown in (VI.3).

$$\frac{\partial}{\partial z} v(z, t) = -L\frac{\partial}{\partial t} i(z, t) - Ri(z, t) \tag{VI.3}$$

Equations (VI.2) and (VI.3) are two couple first order partial differential equations. In order to solves these equations, two boundary conditions must be given along with the initial voltage and current conditions. The two boundary conditions can be any combination of the following four conditions, the current at either end of the line or the voltage at either end of the line.

Now that the equations modelling a single-phase transmission line have been discussed, the equations characterizing the three-phase case will be presented. These equations can be written as

$$\frac{\partial}{\partial z} \mathbf{i}(z, t) = -\mathbf{G}\mathbf{v}(z, t) - \mathbf{C}\frac{\partial}{\partial t} \mathbf{v}(z, t) \tag{VI.4}$$

$$\frac{\partial}{\partial z} \mathbf{v}(z, t) = -\mathbf{R}\mathbf{i}(z, t) - \mathbf{L}\frac{\partial}{\partial t} \mathbf{i}(z, t) \tag{VI.5}$$

where v and **i** are three by one vectors corresponding to the a,b, and c phase-to-ground voltage and the a,b, and c phase current, respectively. R is a three by three diagonal matrix with the diagonal entries corresponding to the phase resistance. If the phase conductors are identical, R is a scalar quantity R times the identity matrix. G, C, and L are all symmetrical three by three matrices corresponding to the three-phase conductance, capacitance, and inductance, respectively. Similar to the single-phase case, equations (VI.4) and (VI.5) can be solved given two boundary conditions and the initial conditions of the transmission lines.

To solve the three-phase transmission line equations it is helpful to transform the variables from the time domain to the frequency domain using the Fourier transform. Once the current and voltage have been transformed, equations **(VI.4)** and **(VI.5)** yield

$$\frac{d}{dz}\mathbf{i}(z,\omega) = -\mathbf{Y}(\omega)\mathbf{v}(z,\omega) \tag{VI.6}$$

$$\frac{d}{dz}\mathbf{v}(z,\omega) = -\mathbf{Z}(\omega)\mathbf{i}(z,\omega) \tag{VI.7}$$

where

$$\mathbf{Y}(\omega) = \mathbf{G} + j\omega\mathbf{C} \tag{VI.8}$$

$$\mathbf{Z}(\omega) = \mathbf{R} + j\omega\mathbf{L} \tag{VI.9}$$

By differentiating both sides of equation **(VI.7)** and substituting equation **(VI.6)** in for $\frac{\mathbf{d}}{\mathbf{dz}}\mathbf{i}(z, \mathbf{o})$, a second order differential equation for the voltage can be obtained.

$$\frac{d^2}{dz^2}\mathbf{v}(z,\omega) = \mathbf{Z}(\omega)\mathbf{Y}(\omega)\mathbf{v}(z,\omega) \tag{VI.10}$$

Similarly, it can be shown that

$$\frac{\mathbf{d}^2}{\mathbf{dz}^2}\mathbf{i}(z,\omega) = \mathbf{Y}(\omega)\mathbf{Z}(\omega)\mathbf{i}(z,\mathbf{o}) \tag{VI.11}$$

In order to solve these equations, first a modal current and voltage will be defined such that the resulting equations will be a set of uncoupled second order equations.

$$\mathbf{v}(z,\omega) = \mathbf{S}\mathbf{v}_\mathbf{m}(z,\omega) \tag{VI.12}$$

$$\mathbf{i}(z,\mathbf{o}) = \mathbf{Q}\mathbf{i}_\mathbf{m}(z,\mathbf{o}) \tag{VI.13}$$

By selecting the columns of **S** and the rows of **Q** to be the eigenvectors of LC and by neglecting the small coupling from the LG, RC, and RG matrices, equations **(VI.10)** and **(VI.11)** can be represented as three scalar second order differential equation

$$\frac{d^2}{dz^2}\mathbf{i}_\mathbf{m}(z,\omega) = \mathbf{A}^2\mathbf{i}_\mathbf{m}(z,\mathbf{o}) \tag{VI.14}$$

$$\frac{d^2}{dz^2}\mathbf{v}_\mathbf{m}(z,\omega) = \Lambda^2\mathbf{v}_\mathbf{m}(z,\omega) \tag{VI.15}$$

where Λ^2 is a diagonal matrix with

$$[\Lambda^2]_{ii} = [\gamma_i + j\omega\lambda_i]2 \tag{VI.16}$$

This yields a general solution

$$\mathbf{i}_m(z,\omega) = \mathbf{i}_m^i(z,\omega) + \mathbf{i}_m^r(z,\omega) = e^{-\Lambda(z-z_o)}\mathbf{i}_m^i(z_o,\omega) + e^{\Lambda(z-z_o)}\mathbf{i}_m^r(z_o,\omega) \tag{VI.17}$$

$$\mathbf{v}_m(z,o) = \mathbf{v}_m^i(z,o) + \mathbf{v}_m^r(z,o) = e^{-\Lambda(z-z_o)}\mathbf{v}_m^i(z,o) + e^{\Lambda(z-z_o)}\mathbf{v}_m^r(z,\omega) \tag{VI.18}$$

where the i superscript denotes the incident component of the solution and the r superscript denotes the reflected component.

To solve the boundary value problem the following relationship is derived by solving equation (VI.7) in terms of the modal voltages and currents.

$$\mathbf{v}_m(z,o) = \mathbf{Z}_c e^{-\Lambda(z-z_o)}\mathbf{i}_m^i(z_o,\omega) - \mathbf{Z}_c e^{\Lambda(z-z_o)}\mathbf{i}_m^r(z_o,\omega) \tag{VI.19}$$

where $\mathbf{Z}_c$ is called the modal characteristic impedance matrix and defined as

$$\mathbf{Z}_c = \mathbf{S}^{-1}\mathbf{Z}(\omega)\mathbf{Q}\Lambda^{-1} \tag{VI.20}$$

This relationship relates the modal voltage to the modal current at z_o. Now the modal voltage at $z=0$ assuming $z_o = 0$ can be solved.

$$\mathbf{v}_{mL}(t) = \mathbf{Z}_c\mathbf{i}_{mL}^i(t) - \mathbf{Z}_c\mathbf{i}_{mL}^r(t) \tag{VI.21}$$

The subscript L indicates that this is the solution at $z=0$ or the left end of the line. Solving for the reflected component of current and substituting it into equation (VI.17) yields

$$\mathbf{i}_{mL}(t) = 2\mathbf{i}_{mL}^i - \mathbf{Z}_c^{-1}\mathbf{v}_{mL}(t) \tag{VI.22}$$

The same relationship can be derived for the current at the right side of the line with z decreasing to the left.

$$\mathbf{i}_{mR}(t) = 2\mathbf{i}_{mR}^i - \mathbf{Z}_c^{-1}\mathbf{v}_{mR}(t) \tag{VI.23}$$

One can also show that the incident wave on the left side of the line corresponds to the reflected wave on the right side of the line delayed and attenuated by $e^{-\Lambda d}$, where d is the line length.

$$\mathbf{i}^{i}_{mL}(t) = -e^{-Ad}\mathbf{i}^{r}_{mR}(t) \qquad \text{(VI.24)}$$

A similar relationship can be made for the reflected component on the left and the incident component on the right.

$$\mathbf{i}^{i}_{mR}(t) = -e^{-\Lambda d}\mathbf{i}^{r}_{mL}(t) \qquad \text{(VI.25)}$$

Since **A** is diagonal with real and imaginary components as diagonal entries, the diagonal components of $e^{-\Lambda d}$ can be broke down into an attenuation factor α_i and a delay factor $e^{-j\omega\lambda_i d}$. From the previous relationships, the simulation block diagram shown in Figure VI.2 was derived were the phase voltages on the left side of the line and the currents on the right side of the line are the inputs. The outputs of this simulations are the voltages at the right and the currents at the left.

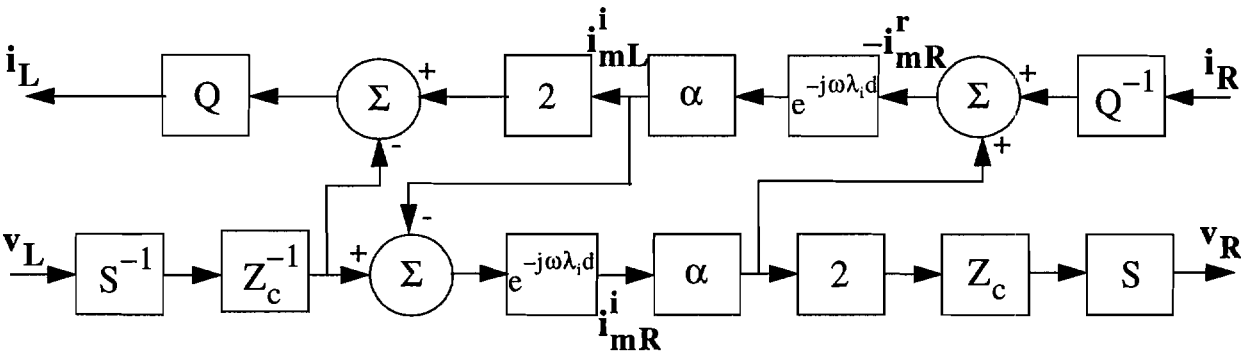

Figure VI.2 Block Diagram for Transmission Line Simulation

VI.5 Transmission Line Transient Study

In this section three different types of pole closure schemes in three-phase transmission lines will be explored. The parameters of the system used in the study are given along with a description of the switching strategies. A comparison of the maximum phase-to-ground and phase-to-phase voltage produced at the open-end of the line for each scheme is made.

The transmission line parameters used in this study are given in Table VI.1 with the physical dimensions of the line shown in Figure VI.3. In this study the transmission lines were open circuited at the receiving end; therefore, the input current at the receiving end was zero. The other input parameter required for the simulation block diagram shown in Figure VI.2 is the input voltage at the source end. This input voltage was assumed to be an ideal three-phase source. The inductance and capacitance matrices were calculated assuming an ideal ground plane.

Initially de-energized 345-kV overhead line
Length of line = 200 miles
Geometrical Mean Radius (GMR) = 0.2245'
Outer Radius = 3.0530''

Table VI.1 Transmission line parameters used in study

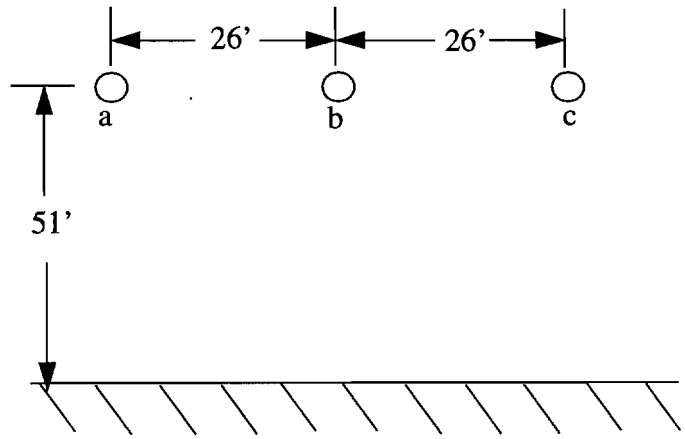

Figure VI.3 Dimensions of transmission lines

The first pole closure scheme simulated was simultaneous pole closure. In this pole closure scheme all phases were closed at the same time. The time used to close all three phases was the

time at which the a-phase voltage was at a positive maximum. The plot of the phase-to-ground voltage at the receiving end for phase a is shown in Figure VI.4. From the plot one can observe that initially the voltage at the receiving end is zero until the voltage wave reaches the receiving end. Once the voltage reaches the receiving end, the reflected voltage causes the voltage to double the initial sending voltage minus losses. Since the loss in the line was 5 percent, the doubled voltage is 1.9 per unit. **A** plot of the phase-to-phase voltage between phases a and c is shown in Figure VI.5. This plot shows that simultaneous pole closure results in a 3.25 per unit phase-to-phase overvoltage.

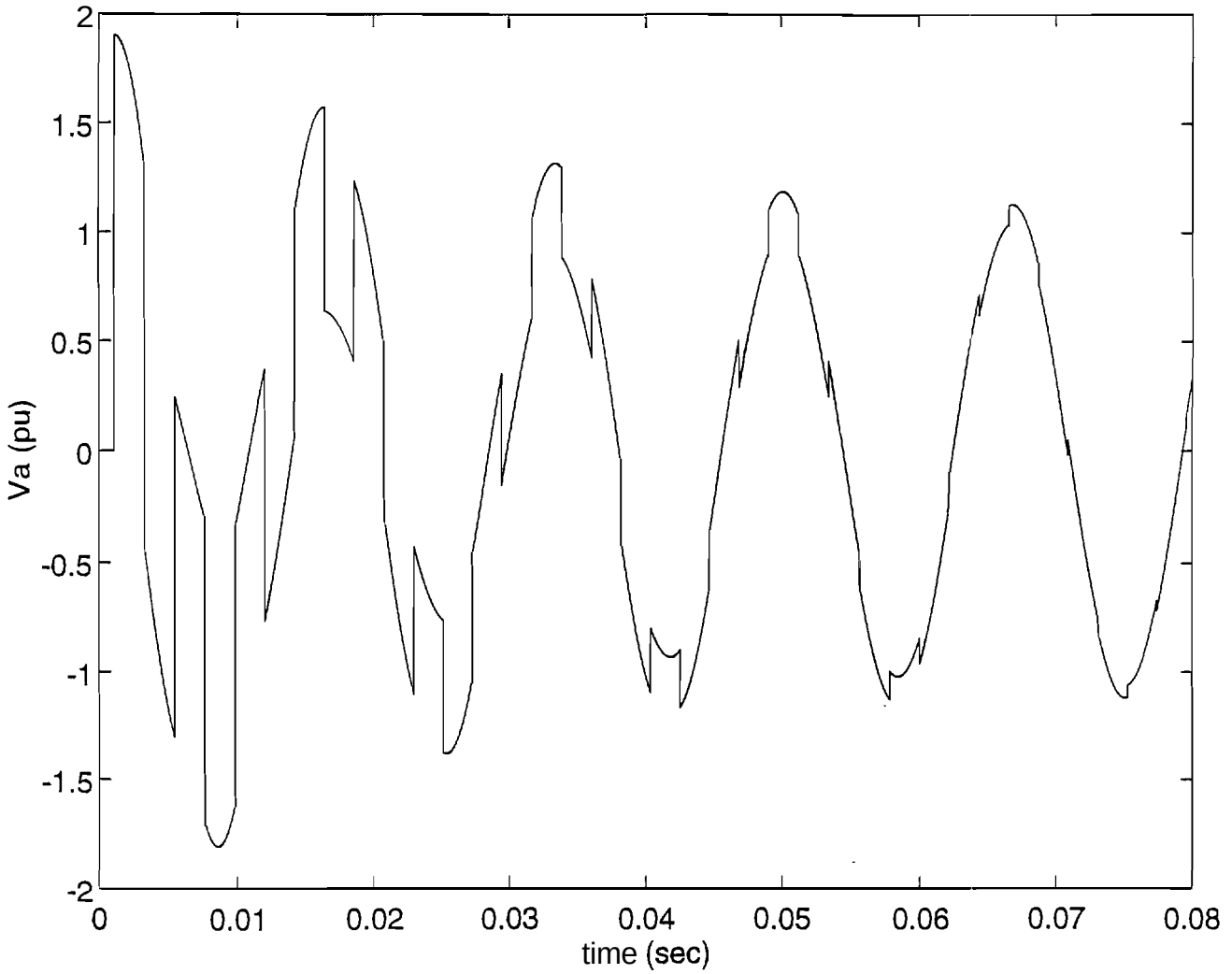

Figure VI.4 Va receiving end for simultaneous pole closure:

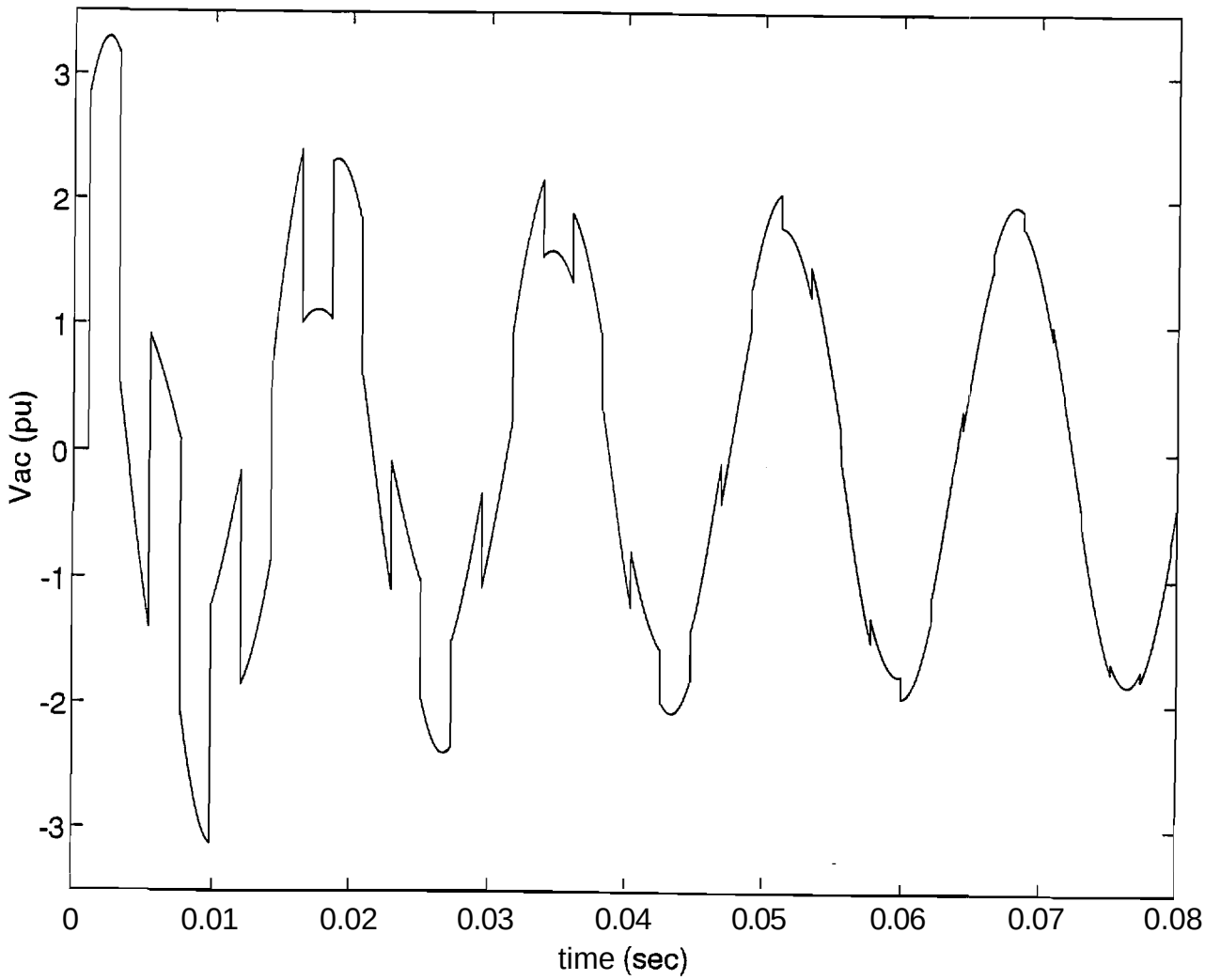

Figure VI.5 Vac receiving end for simultaneous pole closure

Sequential pole closure was the second pole closure scheme simulated. In this scheme the poles were closed on zero crossings of the phase voltage. The time zero closing was when the a phase voltage crossed through zero positively. This was followed by the c phase closure then b. Therefore, this scheme differed from the simultaneous pole close in the fact that the time interval between phase closures were different and the point on the voltage waves where each phase closed was also different. Sequential pole closure produced significantly better results in terms of overvoltages at the receiving end by only having a maximum phase-to-ground voltage of 1.4 per

unit and a maximum phase-to-phase voltage of 2.1 per unit. This substantial reduction reduces the risk of insulator failure due to overvoltage on the line.

The final pole closure scheme to be discussed is maximum voltage pole closure. In maximum voltage pole closure, each phase is closed when the phase voltage is at a maximum. The time zero used in the simulation was when phase a was at a positive maximum. This was followed by the closure of phase c then phase b. This scheme had the same time intervals between phase closures as did the sequential scheme; however, the point on the voltage waveform where the closures occurred differed greatly. This difference resulted in a large increase in the maximum phase-to-ground and phase-to-phase overvoltages produced at the receiving end of the line. The maximum phase-to-ground voltage was 1.9 per unit with the maximum phase-to-phase voltage being 3.4 per unit.

VI.6 Conclusions

Transmission line overvoltages increase the risk of insulator failure. Accurately modeling transmission line overvoltages can help lower the risk of failure and save costs by helping to specify design criteria early in the design. The time interval between phase pole closures and the value of the voltage when the phase closes both affect the phase-to-ground and phase-to-phase overvoltages. Sequential pole closure significantly reduces the maximum overvoltages at the receiving end of the line when compared to simultaneous and maximum voltage pole closure schemes.

References

[1] L. Paris, "Basic considerations of magnitude reduction of switching surges clue to line energization", IEEE Transactions on Power Apparatus and Systems, vol. PAS-87, pp. 295-305, January 1968.

[2] J.P. Bickford, N. Mullineux, and J.R. Reed, Computation of power-system *transients*. London: Institution of Electrical Engineers, 1980, pp. 108-113.

[3] M.M. Morcos and H. Anis, "On the inter-phase energization overvoltages due to random pole closures", Proceedings of the 19th Annual North American Power Symposium, Piscataway, NJ: IEEE, 1987, pp. 417-426

[4] G.L. Wilson and J.G. Kassakian, "Effects of zero sequence modeling and transposition on switching surge overvoltages", IEEE Transactions on Power Apparatus and Systems, vol. PAS-93, pp. 870-877, March/April 1974.

[5] 0 . Wasynczuk, "Class Notes for EE 636", Purdue University, January 1989.

[6] A. Greenwood, Electrical Transients in Power Systems. New York: John Wiley & Sons. 1971. Chapter 6.